EFFECTS OF PRESSURE STRESS WORK AND VISCOUS DISSIPATION IN MIXED CONVECTION FLOW ALONG A VERTICAL FLAT PLATE

by

Mohammad Khairul Bashar
Student No. 100609010P
Registration No. 100609010P
Session: October 2006

MASTER OF PHILOSOPHY
IN
MATHEMATICS

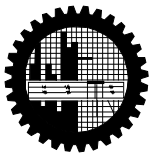

Department of Mathematics
Bangladesh University of Engineering & Technology
Dhaka-1000

The thesis entitled "**Effects of pressure stress work and viscous dissipation in mixed convection flow along a vertical flat plate"** submitted by **Mohammad Khairul Bashar,** Roll : 100609010P, Registration No.100609010P, Session : October 2006 has been accepted as satisfactory in partial fulfilment of the requirement for the degree of Master of Philosophy in Mathematics on 12 th March 2010.

Board of Examiners

(i) **Dr. Md. Mustafa Kamal Chowdhury**. (Supervisor) — Chairman
Professor
Department of Mathematics
BUET, Dhaka-1000

(ii) **Head**(Ex-Officio) — Member
Dept. of Mathematics,
BUET, Dhaka

(iii) **Dr. Md. Manirul Alam Sarker** — Member
Professor
Department of Mathematics
BUET, Dhaka-1000

(iv) **Dr. Md. Abdul Alim** — Member
Associate Professor
Department of Mathematics
BUET, Dhaka-1 000.

(v) **Dr. Sujit Kumer Sen** — Member (External)
Professor
RCMPS
University of Chittagong, Chittagong

Candidate's Declaration

I am hereby declaring that no portion of the work considered in this thesis has been submitted in support of an application for another degree or qualification of this or any other University or Institution of learning either in home or abroad.

_____

Mohammad Khairul Bashar
October 2009

Certificate of Research

This is to certify that the work presented in this thesis is carried out by the author under the supervision of **Dr. Md. Mustafa Kamal Chowdhury**, Professor, Department of Mathematics, Bangladesh University of Engineering & Technology, Dhaka. Bangladesh.

Dr. Md. Mustafa Kamal Chowdhury.

Professor
Department of Mathematics
BUET, Dhaka-1000

Mohammad Khairul Bashar

To my parents and family-
thank you for everything

ACKNOWLEDGEMENT

First and foremost, I wish to express all of my devotion and reverence to the Almighty Allah, most merciful beneficent creator who has enabled me to perform this research work and to submit this thesis.

I wish to thank Dr. Md. Mustafa Kamal Chowdhury, Professor, Department of mathematics, BUET, Dhaka-1000, for his supervision through all stage of this work.1 would also like to thank all other honorable teachers, officers and staffs of this department for their continuous help during the research period.

My sincere thank also goes to Mr. NHM. A. Azim, Assistant Professor, South East University, Dhaka, for his generous help in the computer data acquisition programming and my friends and families for their various kinds of support.

The Author

Abstract

In this study, a mathematical model for steady laminar mixed convection boundary layer flow over a semi infinite, isothermal, vertical flat plate immersed in an incompressible fluid is developed. The governing non linear partial differential equations are first transformed using an appropriate non similar transformation and then solved using an implicit finite difference method with Keller- Box scheme. Numerical results presented include the velocity and temperature profiles as well as the fluid flow and heat transfer characteristics, for the different values of pressure work parameter $\in$, viscous dissipation parameter Ec and heat generation parameter Q while Prandtl number Pr and the buoyancy force parameter Ri are fixed which are taken 1 and 0.72 respectively. The numerical code have been developed using FORTRAN language software. Next, the solution have been showed graphically.

Table of Contents

Contents

Nomenclature

Symbol Meaning

C_{fx}	Skin friction coefficient
C_p	Specific heat
Ec	Eckert number
f	Dimensionless stream function
g	Acceleration due to gravity
L	Reference length
Nu	Nusselt number
P	Hydrostatic pressure
Pr	Prandtl number
Q	Heat generation parameter
q	Heat transfer rate.
Re	Reynold number
R_i	Richardson number.
T_s	Temperature of the surface.
T_∞	Temperature of the ambient fluid
t_r	Temperature ratio
U_∞	Ambient fluid velocity
u, v	Velocity components
x, y	Cartesian coordinates

Greek Symbol

ψ	Dimensionless stream function
•	Thermal conductivity
ρ	Density of the fluid
ν	Kinematic viscosity
μ	Viscosity of the fluid
θ	Dimensionless temperature
ε	Pressure work parameter
β	Co-efficient of thermal expansion
ξ, η	Dimensionless coordinates

List of Figure

page No.

List of Table

CHAPTER 1

INTRODUCTION

1.1 General Introduction

The convective mode of heat transfer is generally divided into two basic processes, namely natural or free convection, and forced convection. In several practical applications, temperature difference exist in the boundary region near a heated or cooled surface. The temperature differences cause density gradients in the fluid medium, and in the presence of a body force such as gravity, free convection effects arise. The density difference gives rise to buoyancy forces. If the motion of the fluid arises from an external agent, then the process is termed forced convection, and the externally imposed flow is generally known. Thus, in any forced convection situation, free convection effects are also present under the presence of gravitational body forces. In addition, when the effect of the buoyancy force in forced convection, or the effect of forced flow in free convection becomes significant, then the process is called mixed convection flows, or combined forced and free convection flows. The effect is especially pronounced in situations where the forced flow velocity is low and/ or the temperature difference is large. In mixed convection flows, the free convection effects and the forced convection effects are of comparable magnitude [28].

The domain of mixed convection regime is generally defined as the region $a \le Gr/\mathrm{Re}^n \le b$, where the Grashof number (Gr) is a measure of the ratio of buoyancy to viscous forces and Reynolds number (Re) indicates the ratio of inertia to viscous forces. The buoyancy parameter Gr/Re^n, provides a measure of the influence of free convection in comparison with that of forced convection on the flow.

The exponent n depends on the flow configuration and the surface heating condition. Outside the mixed convection region $(a \le Gr/\mathrm{Re}^n \le b)$, either the pure forced convection or the pure free convection analysis can be used to describe accurately the flow or the temperature field. As this non- dimensional ratio approaches zero, forced convection dominates; as it approaches infinity, natural convection dominates. Mixed convection may be aiding or opposed. Aiding implies free stream flow in the direction of buoyancy forces; opposed convection implies free stream flow opposite to buoyancy forces.

Convective heat transfer can also be classified as either bounded or unbounded, which is more commonly known as internal or external flow, respectively. Both the free and mixed convection processes may be divided into external flow over immersed body (such as flat plates, cylinders and spheres), and internal flow in ducts (such as pipes, channels and enclosures). The resultant flow can further be classified as either laminar (stable) or turbulent (unstable) flow. The laminar flow is smooth, with a particle of fluid moving steadily in a smooth line parallel to the surface, and a thin layer of fluid then moves as a lamination. On the other hand, the turbulent flow is described as an erratic and chaotic flow with a particle of fluid moving unsteadily in an unpredictable zigzag path. Turbulent flow is generally expected to occur when Reynolds number is high while laminar flow is when Reynolds number is low [21].

Mixed convection flow past a vertical semi infinite flat plate has received much attention and is important in situations encountered in the areas of geothermal power generation and drilling operation, when the free stream velocity and the induced buoyancy velocity are comparable. It continues to be one of the most important problems, also due to its fundamental nature as well as many engineering applications. In spite of the fact that a good number of theoretical and experimental studies were carried out in the past on mixed convection flow, it seems that most of these studies are not on Pure mixed convection $(Gr/\mathrm{Re}^n = 1)$ flows and these are away from the effects of viscous dissipation, pressure work and heat generation together. The viscous dissipation term is always positive and represents a source of heat due to friction between the fluid particles. A variety of expressions are used in the literature for this term like viscous heating, share stress heating and viscous work. The pressure work is the work that required pushing fluid into or out of a control volume. When fluid cross a control surface and enters the

control volume, it must push back the fluid that is already inside the control volume. Since that fluid has a pressure, the entering fluid must do work to move it. For example, rising air expands because as it rises there is less atmospheric pressure compressing it and as it expands becomes cooler. This phenomenon is called adiabatic cooling. The reverse case happens when air sinks. This phenomenon is called adiabatic heating. The viscous dissipation tends to rise the fluid temperature while the pressure work tends to lower its temperature in the upward flow. Literatures and published works on these topics are also reviewed in the next chapters corresponding to the problems.

The present study considers the problem of mixed convection boundary layer flow over a semi infinite vertical flat plate, using air as a working fluid. In this study, the flow is assumed to be laminar, the external flow is considered and steady state prevails. Boundary conditions are discussed on constant surface temperature. The analysis include (i) formulation of the mathematical model to obtain the governing boundary layer flow and heat transfer equations (ii) nonsimilar boundary layer transformation and (iii) numerical computation using a finite difference scheme. The scheme employed is the Box method developed by Keller [14], and throughout the whole course of this study, the main reference for the Keller-box method is the book by Cebeci and Bradshaw [3].

1.2 Objectives of present study

The objectives of the present study are to construct mathematical models, to carry out mathematical formulations and analyses and to develop numerical algorithms for the computations of the following two problems.

- The effects of pressure stress work and viscous dissipation in mixed convection flow of a viscous incompressible fluid past a semi- infinite vertical flat plate.

- The effect of heat generation in mixed convection flow of a viscous incompressible fluid past a semi- infinite vertical flat plate in presence of pressure stress work and viscous dissipation.

Solutions are obtained and analyzed in terms of velocity and temperature profiles, local skin-friction coefficients and the local Nusselt number for different values of Prandtl number Pr , Eckert number Ec , pressure work parameter ε and heat generation parameter Q. The results are also shown graphically.

1.3 Outline of this study

This thesis is divided into three chapters including this introductory one. This chapter should be regarded as preliminaries with general introduction and objectives. In this study, the problems of steady laminar mixed convection boundary layer flows over a semi infinite vertical flat plate with constant surface temperature is considered using air as a working fluid. These problems are generally divided into the two main chapters, namely Chapter 2 and Chapter 3.

Chapter 2 represents the effects of pressure stress work and viscous dissipation in mixed convection flow along a semi- infinite vertical flat plate. Here also discussed on Prandtl number. Since most of the researcher discussed or investigated the effects of viscous dissipation, mainly the effect of pressure work in presence of viscous dissipation is investigated here.

Chapter 3 represents the effect of heat generation in mixed convection flow of a viscous incompressible fluid past a semi- infinite vertical flat plate in presence of pressure stress work and viscous dissipation. Effects of the including parameters, namely heat generation parameter, pressure work parameter and viscous dissipation parameter are discussed taking Prandtl number as 0.72 which corresponds to air.

CHAPTER 2

EFFECTS OF PRESSURE STRESS WORK AND VISCOUS DISSIPATION IN MIXED CONVECTION FLOW ALONG A VERTICAL FLAT PLATE

2.1 Introduction:

The study of mixed convection flow for an incompressible viscous fluid past a heated surface has attracted the interest of many researchers in view of its important applications to many engineering problems which include nuclear reactors cooled during emergency shutdown, electronics devices cooled by fans, heat exchangers placed in a low velocity environment and solar central receivers exposed to wind currents. There are certain situations where the free as well as the forced convection are of comparable magnitude. One such case is when air is flowing over a heated surface at a low velocity. The ratio $Ri(=Gr/\mathrm{Re}^2)$, buoyancy force parameter is used to check the relative magnitudes of forced and free convection according to the criteria

Free convection neglected if $Gr/\mathrm{Re}^2 << 1$

Free and Forced convection comparable if $Gr/\mathrm{Re}^2 \approx 1$

Forced convection neglected if $Gr/\mathrm{Re}^2 >> 1$

In the study of fluid over heated or cooled surfaces, the effect of buoyancy forces neglected when the flow is horizontal. For vertical or inclined surfaces, the buoyancy force modifies the flow field and hence the heat transfer rate. Therefore it is not possible to neglect the effect of buoyancy forces for vertical or inclined heated or cooled surfaces. In recent years, much attention has been paid to develop efficient energy systems. Kumari and Nath [15] developed

the mixed convection flow over a vertical plate due to an impulsive motion. Hossain and Arbad [7] studied the forced and free convection flow past a semi- infinite vertical plate with viscous dissipation effects using the method of parametric differentiation. Yao [26] studied the mixed convection flow along a vertical flat plate. It has been generally recognized that Gr/Re^2 is the governing parameter for the convection flow along a vertical plate.

In almost all heat convection studies, the viscous dissipation and pressure stress terms are neglected in the energy equation. Some researchers like Joshi and Gebhart [13] studied the effect of pressure stress work and viscous dissipation in some natural convection flows. Alam et al. [1] studied the same with heat conduction along a vertical flat plate. Zakerullah [27] investigated the viscous dissipation and pressure work effects in axisymmetric natural convection flows. Miyamoto et al [18] also investigated the effect of axial heat conduction in a vertical flat plate on free convection heat transfer. Gebhart [4] studied the flow generated by the plate surface temperature varying as power of x (the distance measuring along the plate surface from the leading edge) by a series expansion method and Gebhart and Mollendorf [5] derived similarity solutions for such a flow generated by the plate surface temperature varying exponentially with x.

In the present study, the effects of pressure stress work and viscous dissipation in mixed convection flow of a viscous incompressible fluid past a semi- infinite vertical flat plate are investigated. This investigation is on the steady mixed convection flow over a heated vertical flat plate. To obtain the solution of the governing equations for this case, we direct our attention to the region near the leading edge of the plate. The steadiness is induced by impulsively creating motion in the ambient fluid and at the same time suddenly raising the wall temperature above the surrounding temperature. The solutions of the nonlinear coupled singular parabolic partial differential equations governing the steady mixed convection flow are obtained numerically by using an implicit finite difference scheme. Though for an incompressible fluid, the value of the Eckert number Ec is less than unity, its effect on the temperature and flow fluids cannot be neglected (Gebhart [4] and Gebhart and Mollendorf [5]).The result will be obtained for different values of relevant physical parameters and will be shown graphically as well as in tables.

2.2 Geometry of the problem:

A semi-infinite vertical plate is placed in an ambient viscous fluid with uniform temperature T_∞. The temperature of the plate is the same as that of the ambient fluid. At time t = 0, the ambient fluid is impulsively moved with a constant velocity U_∞ and at the same time the surface temperature is suddenly raised to T_s ($T_s > T_\infty$). Fig. 1 shows the flow field over a vertical surface, where x is the distance along the surface of the plate measured from the leading edge x=0 and y is the distance normal to the surface. The buoyancy force arises due to the temperature difference between the surface and the fluid. u and v denoting respectively the velocity components in the x and y direction.

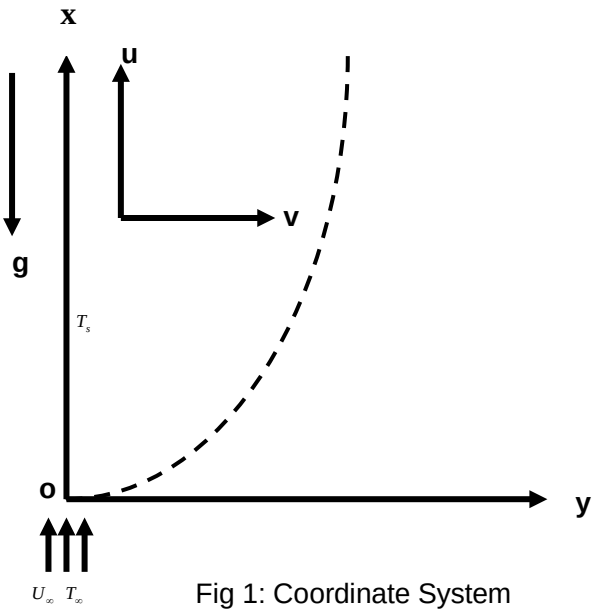

Fig 1: Coordinate System

For steady two dimensional flow the boundary layer equations including viscous dissipation and pressure work are

Continuity equation

$$\frac{\partial u}{\partial x}+\frac{\partial v}{\partial y}=0 \tag{2.2.1}$$

Momentum equation

$$u\frac{\partial u}{\partial x}+v\frac{\partial u}{\partial y}=\nu\frac{\partial^2 u}{\partial y^2}+\beta g(T-T_\infty) \tag{2.2.2}$$

and the Energy equation

$$u\frac{\partial T}{\partial x}+v\frac{\partial T}{\partial y}=\frac{\kappa}{\rho C_P}\frac{\partial^2 T}{\partial y^2}+\frac{\nu}{C_P}\left(\frac{\partial u}{\partial y}\right)^2+\frac{T\beta}{\rho C_P}u\frac{\partial P}{\partial x} \tag{2.2.3}$$

The boundary conditions for the present problem are

$$\left.\begin{array}{l} \mathrm{u}=0,\mathrm{v}=0,\mathrm{T}=\mathrm{T_s}\ \ at\ y=0 \\ u\to U_\infty, T\to T_\infty\ as\ y\to\infty \end{array}\right\} \tag{2.2.4}$$

where T is the fluid temperature, • is the kinematic viscosity, • is the fluid expansion coefficient, g is the acceleration due to gravity, • is the thermal conductivity, C_p is the specific heat at constant pressure, • is the fluid density and P is the pressure. The last two terms in the energy equation are the viscous dissipation and the pressure stress work respectively. The fluid pressure consists of the hydrostatic and motion pressure.

The motion pressure is considered small compared to hydrostatic pressure and is ignored. For the hydrostatic pressure we have

$$\frac{dP}{dx}=-\rho g \tag{2.2.5}$$

The viscous dissipation term is always positive and represents a source of heat due to friction between the fluid particles. The pressure work is the work required to push fluid into or out of a control volume. The viscous dissipation tends to raise the fluid temperature while the pressure work tends to lower its temperature in the upward flow examined here.

2.3 Transformation of the governing equations:

The following transformations for the independent and dependent variables are introduced in equations (2.2.1) to (2.2.3).

$$\psi(x,y)=\sqrt{U_\infty \nu x}\, f(\xi,\eta), \qquad \eta = y\sqrt{\frac{U_\infty}{\nu x}}, \qquad \xi = \frac{x}{L}Ri, \qquad \theta(\xi,\eta)=\frac{T(x,y)-T_\infty}{T_s-T_\infty}$$

Here • is the dimensionless similarity variable, L denoting the reference length and • is the stream function which satisfies the equation of continuity and $u=\frac{\partial \psi}{\partial y}, v=-\frac{\partial \psi}{\partial x}$, $\theta(\xi,\eta)$ is the dimensionless temperature.

Now we get the non-dimensional momentum and energy equations as

$$f'''+\frac{1}{2}ff''+\theta\xi=\xi\left(f'\frac{\partial f'}{\partial \xi}-f''\frac{\partial f}{\partial \xi}\right) \qquad (2.3.1)$$

$$\frac{1}{\mathrm{Pr}}\theta''+\frac{1}{2}f\theta'+Ecf''^2-\varepsilon\xi\left(f'\theta+\frac{T_\infty}{T_s-T_\infty}f'\right) = \xi\left(f'\frac{\partial \theta}{\partial \xi}-\theta'\frac{\partial f}{\partial \xi}\right) \qquad (2.3.2)$$

where $\mathrm{Pr}=\frac{\rho\nu C_p}{\kappa}$ is the Prandtl number, Eckert number $Ec=\frac{U_\infty{}^2}{C_p(T_s-T_\infty)}$ is treated as viscous dissipation parameter which is less than unity and the pressure work parameter $\varepsilon=\frac{\beta g L}{C_p Ri}$ which is also less than unity. $Ri=\frac{Gr}{\mathrm{Re}^2}=\frac{\beta g(T_s-T_\infty)L}{U_\infty^2}$ is the buoyancy force parameter whose value is taken unity for this problem.

In the above equations the primes denote differentiation with respect to •.

The corresponding boundary condition takes the form

$$\left.\begin{array}{llll} f=0, & f'=0, & \theta=1 & at\ \ \eta=0 \\ f'\to 1, & \theta\to 0 & as & \eta\to\infty \end{array}\right\} \qquad (2.3.3)$$

2.4 Solution Methodology:

To get the solutions of the differential equations (2.3.1) and (2.3.2) along with the boundary condition (2.3.3), we shall employ a most practical, an efficient and accurate solution technique, known as implicit finite difference method together with Keller-box elimination technique which is well documented and widely used by Keller and Cebeci and recently by Hossain and Alim.

To apply the aforementioned method, we first convert the equations (2.3.1) and (2.3.2) into the following system of first order differential equations with dependent variables $u(\xi,\eta)$, $v(\xi,\eta)$ and $p(\xi,\eta)$ along with the boundary condition (2.3.3) as

$$f' = u \tag{2.4.1}$$

$$f'' = u' = v \tag{2.4.2}$$

$$f''' = u'' = v' \tag{2.4.3}$$

$$\theta' = p \tag{2.4.4}$$

$$\theta'' = p' \tag{2.4.5}$$

Equations (2.3.1) and (2.3.2) transform to

$$v' + p_1 fv + p_3\theta = \xi\left(u\frac{\partial u}{\partial \xi} - v\frac{\partial f}{\partial \xi}\right) \tag{2.4.6}$$

$$\frac{1}{\Pr}p' + p_1 fp + p_2 v^2 - p_4 u\theta - p_5 u = \xi\left(u\frac{\partial \theta}{\partial \xi} - p\frac{\partial f}{\partial \xi}\right) \tag{2.4.7}$$

where

$$p_1 = \frac{1}{2},\ p_2 = Ec,\ p_3 = \xi,\quad p_4 = \varepsilon\xi,\quad p_5 = \in \xi\, t_r,\quad t_r = \frac{T_\infty}{T_s - T_\infty} \tag{2.4.8}$$

The boundary conditions are:

$$\left.\begin{aligned} f = 0,\quad f' = u = 0,\quad \theta = 1 \quad at\ \ \eta = 0 \\ f' = u \to 1,\quad \theta \to 0 \quad as\ \ \eta \to \infty \end{aligned}\right\} \tag{2.4.9}$$

We now consider the net rectangle on the (•, •) plane shown in the figure (2) and denote the net points by

$$\left.\begin{aligned} &\xi^0 = 0, \quad \xi^i = \xi^{i-1} + k_i \quad where \quad i = 1,2,\ldots N \\ &\eta_0 = 0, \quad \eta_j = \eta_{j-1} + h_j \quad where \quad j = 1,2,\ldots J \end{aligned}\right\} \tag{2.4.10}$$

Here 'n' and 'j' are just sequence of numbers on the *(• , •)* plane , k_i and h_j are the variable mesh widths.

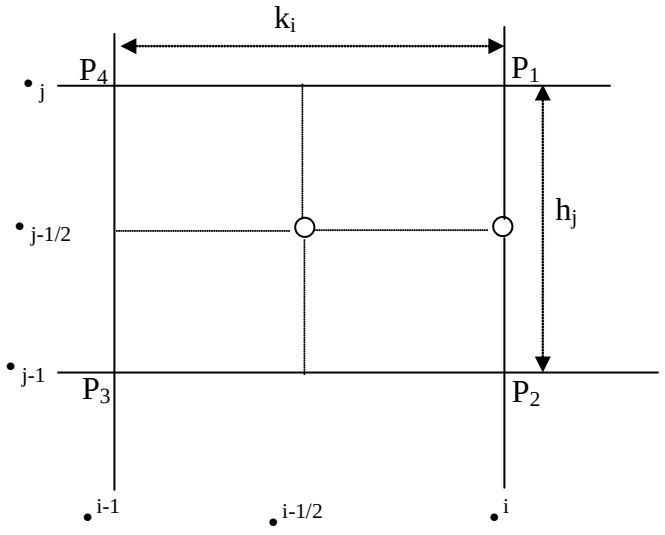

Figure 2: Net rectangle of the difference approximation for the Box scheme.

We approximate the quantities (f, u, v, p) at the points ($\bullet^i$, $\bullet_j$) of the net by($f_j^i, u_j^i \;\; v_j^i, \;\; p_j^i$) which we call net function . We also employ the notation g_j^i for the quantities midway between net points shown in figure (2) and for any net function as

$$\xi^{i-1/2} = \frac{1}{2}(\xi^i + \xi^{i-1}) \tag{2.4.11a}$$

$$\eta_{j-1/2} = \frac{1}{2}(\eta_j + \eta_{j-1}) \tag{2.4.11b}$$

$$\theta_j^{\,i-1/2} = \frac{1}{2}(\theta_j^{\,i} + \theta_j^{\,i-1}) \tag{2.4.11c}$$

$$\theta_{j-1/2}^{i} = \frac{1}{2}(\theta_j^{\,i} + \theta_{j-1}^{i}) \tag{2.4.11d}$$

Now we write the difference equations that are to approximate the three first order ordinary differential equations (2.4.1),(2.4.2) and (2.4.4) according to Box method by considering one mesh rectangle. We start by writing the finite difference approximation of the above three equations using central difference quotients and average about the mid-point $(\xi^i, \eta_{j-1/2})$ of the segment P_1P_2 shown in the figure (2) and the finite difference approximations to the two first order differential equations (2.4.6)-(2.4.7) are written for the mid point $(\xi^{i-1/2}, \eta_{j-1/2})$ of the rectangle $P_1P_2P_3P_4$. This procedure yields.

$$h_j^{-1}(f_j^i - f_{j-1}^i) = u_{j-1/2}^i = \frac{u_{j-1}^i + u_j^i}{2} \tag{2.4.12}$$

$$h_j^{-1}(u_j^i - u_{j-1}^i) = v_{j-1/2}^i = \frac{v_{j-1}^i + v_j^i}{2} \tag{2.4.13}$$

$$h_j^{-1}(\theta_j^i - \theta_{j-1}^i) = p_{j-1/2}^i = \frac{p_{j-1}^i + p_j^i}{2} \tag{2.4.14}$$

$$\begin{aligned} &\frac{v_j^i - v_{j-1}^i}{h_j} + \frac{v_j^{i-1} - v_{j-1}^{i-1}}{h_j} + p_1(fv)_{j-1/2}^i + p_1(fv)_{j-1/2}^{i-1} + p_3(\theta)_{j-1/2}^i + p_3(\theta)_{j-1/2}^{i-1} \\ &= \alpha_i\left[(u^2)_{j-1/2}^i - (u^2)_{j-1/2}^{i-1} - (fv)_{j-1/2}^i + v_{j-1/2}^i f_{j-1/2}^{i-1} - v_{j-1/2}^{i-1} f_{j-1/2}^i + (fv)_{j-1/2}^{i-1}\right] \end{aligned} \tag{2.4.15}$$

$$\begin{aligned} &\frac{1}{\Pr h_j}(p_j^i - p_{j-i}^i) + p_1(fp)_{j-1/2}^i + p_2(v^2)_{j-1/2}^i - p_4(u\theta)_{j-1/2}^i - p_5 u_{j-1/2}^i - \alpha_i(u\theta)_{j-1/2}^i + \alpha_i(fp)_{j-1/2}^i \\ &= \alpha_i\left[-u_{j-1/2}^i \theta_{j-1/2}^{i-1} + u_{j-1/2}^{i-1}\theta_{j-1/2}^i - (u\theta)_{j-1/2}^{i-1} + p_{j-1/2}^i f_{j-1/2}^{i-1} - f_{j-1/2}^i p_{j-1/2}^{i-1} + (pf)_{j-1/2}^{i-1}\right] \\ &- \frac{1}{\Pr h_j}(p_j^{i-1} - p_{j-i}^{i-1}) - p_1(fp)_{j-1/2}^{i-1} - p_2(v^2)_{j-1/2}^{i-1} + p_4(u\theta)_{j-1/2}^{i-1} + p_5 u_{j-1/2}^{i-1} \end{aligned} \tag{2.4.16}$$

where $\alpha_i = \frac{1}{k_i}\xi_{j-1/2}^{i-1/2}$

Now from the equation (2.4.15) we get

$$\frac{v_j^i - v_{j-1}^i}{h_j} + \frac{v_j^{i-1} - v_{j-1}^{i-1}}{h_j} + (p_1 + \alpha_i)(fv)_{j-1/2}^i - \alpha_i (u^2)_{j-1/2}^i + p_3 (\theta)_{j-1/2}^i$$
$$+ \alpha_i (v_{j-1/2}^{i-1} f_{j-1/2}^i - v_{j-1/2}^i f_{j-1/2}^{i-1}) = R_{j-1/2}^{i-1} \qquad (2.4.17)$$

where $R_{j-1/2}^{i-1} = -L_{j-1/2}^{i-1} + \alpha_i \left[(fv)_{j-1/2}^{i-1} - (u^2)_{j-1/2}^{i-1} \right]$

and $L_{j-1/2}^{i-1} = \frac{v_j^{i-1} - v_{j-1}^{i-1}}{h_j} + p_1 (fv)_{j-1/2}^{i-1} + p_3 \theta_{j-1/2}^{i-1}$

Again from the equation (2.4.16) we get

$$\frac{1}{\mathrm{Pr}} \frac{p_j^i - p_{j-1}^i}{h_j} + (p_1 + \alpha_i)(fp)_{j-1/2}^i + p_2 (v^2)_{j-1/2}^i - (p_4 + \alpha_i)(u\theta)_{j-1/2}^i + p_5 u_{j-1/2}^i$$
$$- \alpha_i (u_{j-1/2}^{i-1} \theta_{j-1/2}^i - u_{j-1/2}^i \theta_{j-1/2}^{i-1} + f_{j-1/2}^{i-1} p_{j-1/2}^i - f_{j-1/2}^i p_{j-1/2}^{i-1}) = T_{j-1/2}^{i-1} \qquad (2.4.18)$$

where $T_{j-1/2}^{i-1} = -M_{j-1/2}^{i-1} + \alpha_i \left[(fp)_{j-1/2}^{i-1} - (u\theta)_{j-1/2}^{i-1} \right]$

and $M_{j-1/2}^{i-1} = \frac{1}{\mathrm{Pr}} \frac{p_j^{i-1} - p_{j-1}^{i-1}}{h_j} + p_1 (fp)_{j-1/2}^{i-1} + p_2 (v^2)_{j-1/2}^{i-1}$
$$- p_4 (u\theta)_{j-1/2}^{i-1} - p_5 u_{j-1/2}^{i-1}$$

The boundary conditions become

$$f_0^i = 0, \quad u_0^i = 0, \quad \theta_0^i = 1 \qquad (2.4.19)$$
$$u_J^i = 0, \quad \theta_J^i = 0$$

If we assume $f_j^{i-1}, u_j^{i-1}, v_j^{i-1}, \theta_j^{i-1}, p_j^{i-1}$ to be known for $0 \le j \le J$, equations (2.4.12) to (2.4.14) and (2.4.17) to (2.4.19) form a system of 5J + 5 non linear equations for the solutions of the 5J + 5 unknowns ($f_j^i, u_j^i, v_j^i, \theta_j^i, p_j^i$) , j = 0,1,2 …J. These non linear system of algebraic equations are to be linearized by Newton's Quassy linearization method . We define the iterates

[f_j^i, u_j^i, v_j^i, θ_j^i, p_j^i] , i = 0,1,2 …IMAX with initial values equal those at the previous x-station, which are usually the best initial guess availables. For the higher iterates we set:

$$f_j^{(i+1)} = f_j^{(i)} + \delta f_j^{(i)} \tag{2.4.20}$$

$$u_j^{(i+1)} = u_j^{(i)} + \delta u_j^{(i)} \tag{2.4.21}$$

$$v_j^{(i+1)} = v_j^{(i)} + \delta v_j^{(i)} \tag{2.4.22}$$

$$\theta_j^{(i+1)} = \theta_j^{(i)} + \delta \theta_j^{(i)} \tag{2.4.23}$$

$$p_j^{(i+1)} = p_j^{(i)} + \delta p_j^{(i)} \tag{2.4.24}$$

Now we substitute the right hand sides of the above equations in place of f_j^i, u_j^i, v_j^i, θ_j^i and p_j^i in equations (2.4.12) to (2.4.14), (2.4.17) to (2.4.19) and omitting the terms that are quadratic in δf_j^i , δu_j^i, δv_j^i, $\delta \theta_j^i$ and δp_j^i. This procedure yields the following system of algebraic equations:

$$\delta f_j^{(i)} - \delta f_{j-1}^{(i)} - \frac{h_j}{2}(\delta u_j^{(i)} + \delta u_{j-1}^{(i)}) = (r_1)_j \tag{2.4.25}$$

Where $(r_1)_j = f_{j-1}^{(i)} - f_j^{(i)} + h_j u_{j-1/2}^{(i)}$ (2.4.26)

$$\delta u_j^{(i)} - \delta u_{j-1}^{(i)} - \frac{h_j}{2}(\delta v_j^{(i)} + \delta v_{j-1}^{(i)}) = (r_4)_j \tag{2.4.27}$$

$$(r_4)_j = u_{j-1}^{(i)} - u_j^{(i)} + h_j v_{j-1/2}^{(i)} \tag{2.4.28}$$

$$\delta \theta_j^{(i)} - \delta \theta_{j-1}^{(i)} - \frac{h_j}{2}(\delta p_j^{(i)} + \delta p_{j-1}^{(i)}) = (r_5)_j \tag{2.4.29}$$

where $(r_5)_j = \theta_{j-1}^{(i)} - \theta_j^{(i)} + h_j p_{j-1/2}^{(i)}$ (2.4.30)

$$\begin{aligned}&(s_1)_j \delta v_j^{(i)} + (s_2)_j \delta v_{j-1}^{(i)} + (s_3)_j \delta f_j^{(i)} + (s_4)_j \delta f_{j-1}^{(i)} + (s_5)_j \delta u_j^{(i)} \\ &+ (s_6)_j \delta u_{j-1}^{(i)} + (s_7)_j \delta \theta_j^{(i)} + (s_8)_j \delta \theta_{j-1}^{(i)} + (s_9)_j \delta p_j^i + (s_{10})_j \delta p_{j-1}^i = (r_2)_j\end{aligned} \tag{2.4.30}$$

where $(s_1)_j = h_j^{-1} + \frac{1}{2}(p_1 + \alpha_i) f_j^{(i)} - \frac{1}{2}\alpha_i f_{j-1/2}^{i-1}$ (2.4.31)

$$(s_2)_j = -h_j^{-1} + \frac{1}{2}(p_1 + \alpha_i) f_{j-1}^{(i)} - \frac{1}{2}\alpha_i f_{j-1/2}^{i-1} \tag{2.4.32}$$

$$(s_3)_j = \frac{1}{2}(p_1 + \alpha_i) v_j^{(i)} + \frac{1}{2}\alpha_i v_{j-1/2}^{i-1} \tag{2.4.33}$$

$$(s_4)_j = \frac{1}{2}(p_1 + \alpha_i) v_j^{(i)} + \frac{1}{2}\alpha_i v_{j-1/2}^{i-1} \tag{2.4.34}$$

$$(s_5)_j = \alpha_i u_j^{(i)} \tag{2.4.35}$$

$$(s_6)_j = \alpha_i u_{j-1}^{(i)} \tag{2.4.36}$$

$$(s_7)_j = \frac{p_3}{2} \tag{2.4.37}$$

$$(s_8)_j = \frac{p_3}{2} \tag{2.4.38}$$

$$(s_9)_j = 0 \tag{2.4.39}$$

$$(s_{10})_j = 0 \tag{2.4.40}$$

$$(r_2)_j = R_{j-1/2}^{i-1} - h_j^{-1}(v_j^{(i)} - v_{j-1}^{(i)}) - (p_1 + \alpha_i)(fv)_{j-1/2}^{(i)} - \alpha_i (u^2)_{j-1/2}^{(i)} - p_3 \theta_{j-1/2}^{(i)} - \alpha_i f_{j-1/2}^{(i)} v_{j-1/2}^{i-1} + \alpha_i f_{j-1/2}^{i-1} v_{j-1/2}^{(i)} \tag{2.4.41}$$

Here the coefficients $(s_9)_j$ and $(s_{10})_j$, which are zero in this case, are included here for the generality.

Similarly by using the equations (2.4.20) to (2.4.24) in the equation (2.4.18) we get the following form:

$$(t_1)_j \delta p_j^{(i)} + (t_2)_j \delta p_{j-1}^{(i)} + (t_3)_j \delta f_j^{(i)} + (t_4)_j \delta f_{j-1}^{(i)} + (t_5)_j \delta u_j^{(i)} + (t_6)_j \delta u_{j-1}^{(i)} + (t_7)_j \delta \theta_j^{(i)} + (t_8)_j \delta \theta_{j-1}^{(i)} + (t_9)_j \delta v_j^{(i)} + (t_{10})_j \delta v_{j-1}^{(i)} = (r_3)_j \tag{2.4.42}$$

where $(t_1)_j = \frac{1}{P_r} h_j^{-1} + \frac{1}{2} f_j^{(i)} (p_1 + \alpha_i) - \frac{1}{2} \alpha_i f_{j-1/2}^{i-1}$ (2.4.43)

$$(t_2)_j = -\frac{1}{P_r} h_j^{-1} + \frac{1}{2} f_{j-1}^{(i)} (p_1 + \alpha_i) - \frac{1}{2} \alpha_i f_{j-1/2}^{i-1} \tag{2.4.44}$$

$$(t_3)_j = \frac{1}{2} p_j^{(i)} (p_1 + \alpha_i) + \frac{1}{2} \alpha_i p_{j-1/2}^{i-1} \tag{2.4.45}$$

$$(t_4)_j = \frac{1}{2} p_{j-1}^{(i)} (p_1 + \alpha_i) + \frac{1}{2} \alpha_i p_{j-1/2}^{i-1} \tag{2.4.46}$$

$$(t_5)_j = -\frac{1}{2} \theta_j^{(i)} (p_4 + \alpha_i) - \frac{1}{2} p_5 + \frac{1}{2} \alpha_i u_{j-1/2}^{i-1} \tag{2.4.47}$$

$$(t_6)_j = -\frac{1}{2} \theta_{j-1}^{(i)} (p_4 + \alpha_i) - \frac{1}{2} p_5 + \frac{1}{2} \alpha_i u_{j-1/2}^{i-1} \tag{2.4.48}$$

$$(t_7)_j = -\frac{1}{2} u_j^{(i)} (p_4 + \alpha_i) - \frac{1}{2} \alpha_i u_{j-1/2}^{i-1} \tag{2.4.49}$$

$$(t_8)_j = -\frac{1}{2} u_{j-1}^{(i)} (p_4 + \alpha_i) - \frac{1}{2} \alpha_i u_{j-1/2}^{i-1} \tag{2.4.50}$$

$$(t_9)_j = p_2 v_j^{(i)} \tag{2.4.51}$$

$$(t_{10})_j = p_2 v_{j-1}^{(i)} \tag{2.4.52}$$

$$(r_3)_j = T_{j-1/2}^{i-1} - \frac{1}{P_r} h_j^{-1}(p_j^{(i)} - p_{j-1}^{(i)}) - (p_1 + \alpha_{i)})(fp)_{j-1/2}^{(i)} - p_2 (v^2)_{j-1/2}^{(i)} + (p_4 + \alpha_i)(u\theta)_{j-1/2}^{(i)}$$
$$+ p_5 u_{j-1/2}^{(i)} + \alpha_i u_{j-1/2}^{i-1}\theta_{j-1/2}^{(i)} - \alpha_i \theta_{j-1/2}^{i-1} u_{j-1/2}^{(i)} + \alpha_i f_{j-1/2}^{i-1} p_{j-1/2}^{(i)} - \alpha_i p_{j-1/2}^{i-1} f_{j-1/2}^{(i)} \tag{2.4.53}$$

The boundary conditions (2.4.19) become

$$\delta f_0^i = 0,\ \delta u_0^i = 0,\ \delta \theta_0^i = 0,$$
$$\delta u_J^i = 0,\ \delta \theta_J^i = 0 \tag{2.4.54}$$

which just express the requirement for the boundary conditions to remain during the iteration process.

Now the system of linear equations (2.4.25) -(2.4.30), (2.4.41), (2.4.42) and (2.4.53) together with the boundary conditions (2.4.54) can be written in a block matrix from a coefficient matrix, which are solved by modified ‘Keller Box’ methods especially introduced by Keller . Later, this method has been used most efficiently by Cebeci and Bradshow and recently by Hossain . Results are shown in graphical form by using the numerical values obtained from the above technique.

The solutions of the above equations (2.3.1) and (2.3.2) together with the boundary conditions (2.3.3) enable us to calculate the skin friction • and the rate of heat transfer q at the surface in the boundary layer from the following relations:

$$\tau = \mu\left(\frac{\partial u}{\partial y}\right)_{y=0} = \frac{\mu U_\infty}{L}\xi^{-1/2}\sqrt{\frac{Gr}{\mathrm{Re}}}\, f''(\xi,0) \tag{2.4.55}$$

$$q = -k\left(\frac{\partial T}{\partial y}\right)_{y=0} = -k\frac{T_s - T_\infty}{L}\xi^{-1/2}\sqrt{\frac{Gr}{\mathrm{Re}}}\,\theta'(\xi,0) \tag{2.4.56}$$

Hence, the local skin- friction co-efficient and the heat transfer rate in terms of Nusselt number are given by

$$C_f \xi^{1/2}\frac{\mathrm{Re}^{3/2}}{2Gr^{1/2}} = f''(\xi,0) \qquad 2.4.57$$

$$Nu\,\xi^{-1/2}\frac{Gr^{1/2}}{\mathrm{Re}^{3/2}} = -\theta'(\xi,0) \qquad 2.4.58$$

2.5 Result and Discussion:

Equations (2.3.1) and (2.3.2) under condition (2.3.3) have been solved by the implicit finite difference scheme described earlier. In this solution buoyancy force parameter R_i is considered as unity. Investigation has been focused on the neighbouring points of $\xi = 0$, but not at $\xi = 0$. Nevertheless, under consideration of $\xi = 0$ equation (2.3.1) turns to the well known Blassius equation which has the solution $f''(\xi,0) = 0.33201$. In all the tables 2.5f, 2.5g, and 2.5h, the results are found to be in very good agreement with the Blasius solution. The corresponding energy equation in the absent of viscous dissipation and pressure work was solved by Polhausen (1921). For Prandtl numbers ≥ 0.6 i.e. $0.6 \leq \Pr \leq 1$, the dimensionless heat transfer rate was presented by $0.332\,\Pr^{1/3}$. These informations are described elaborately in the book [22]. Our results also match with the Polhausen's result which have been shown in the following table 2.5.a.

Name of the gases	Prandtl no. Pr	Polhausen	Present result
		$-\theta'(\xi,0)$	
Air at 250^0K	0.72	0.29757	0.29563
Methen at 250^0K	0.742	0.30057	0.29882
Helium at 250^0K	0.681	0.29209	0.28981
Water vapor at 380^0K	1.0	0.33200	0.33205

Table 2.5.a: Values of $-\theta'(\xi,0)$ for various values of Pr when Ec=0.0 and $\varepsilon = 0.0$.

As a check on the accuracy of the present numerical scheme, some results are compared with those of Soundalgekar et al. [23], Hossain and Arbad [7] for Pr=0.72 and $\varepsilon = 0.0$ in the following table 2.5.b. We see from the column of Soundalgekar , Hossain and Arbad that increasing of Ec decreases the local heat transfer rate $-\theta'(\xi.0)$ for the fixed buoyancy force parameter R_i=0.1 in the absent of pressure work effect. Similar result is seen from the present work for the fixed buoyancy force parameter R_i=1.

Ec	Soundalgekar	Hossain and Arbad	Present result
	R_i=0.1	R_i=0.1	R_i=1
	$-\theta'(\xi.0)$		
0.0	0.3157	0.3174	0.29563
0.01	0.3141	0.3169	0.29438
0.05	-	-	0.28937
0.1	-	-	0.28311

Table2.5.b: Values of $-\theta'(\xi,0)$ for various values of Ec when Pr=0.72 and $\varepsilon = 0.0$.

Numerical values are presented in the table 2.5c for velocity and temperature profiles for variation of Prandtl number Pr against •. Table 2.5d and 2.5e contain the values of the same factors against • for the variation of ε and Ec respectively.

Values of •	Pr=0.3		Pr=0.72		Pr=1.0		Pr=10.0	
	$f'(\xi,\eta)$	$\theta(\xi,\eta)$	$f'(\xi,\eta)$	$\theta(\xi,\eta)$	$f'(\xi,\eta)$	$\theta(\xi,\eta)$	$f'(\xi,\eta)$	$\theta(\xi,\eta)$
0.00000	0.00000	1.00000	0.00000	1.00000	0.00000	1.00000	0.00000	1.00000
0.02623	0.04428	0.99201	0.03854	0.98917	0.03653	0.98793	0.02474	0.97575
0.05248	0.08782	0.98402	0.07634	0.97832	0.07231	0.97585	0.04875	0.95143
1.77392	1.40519	0.48271	1.17778	0.32772	1.10282	0.26913	0.74703	0.00664
1.82795	1.40588	0.46901	1.17988	0.31225	1.10573	0.25367	0.75758	0.00402
1.93982	1.40266	0.44130	1.18096	0.28166	1.10898	0.22350	0.77859	0.00027

Table 2.5c : Numerical values of the velocity profile and the temperature profile for different values of Prandtl number Pr while Ec=0.01and ε =0.01.

Values of •	ε =0.0		ε =0.01		ε =0.04		ε =0.07	
	$f'(\xi,\eta)$	$\theta(\xi,\eta)$	$f'(\xi,\eta)$	$\theta(\xi,\eta)$	$f'(\xi,\eta)$	$f'(\xi,\eta)$	$f'(\xi,\eta)$	$\theta(\xi,\eta)$
0.00000	0.00000	1.00000	0.00000	1.00000	0.00000	1.00000	0.00000	1.00000
0.02623	0.03877	0.98934	0.03854	0.98917	0.03789	0.98869	0.03728	0.98825
0.10511	0.15075	0.95722	0.14984	0.95655	0.14722	0.95465	0.14479	0.95289
2.97288	1.09818	0.09263	1.09295	0.08910	1.07761	0.07909	1.06278	0.06989
3.05619	1.08961	0.08330	1.08462	0.07989	1.06996	0.07021	1.05575	0.06131
4.23775	1.01583	0.01450	1.01330	0.01232	1.00574	0.00604	0.99824	0.00011

Table 2.5d: Numerical values of the velocity profile and the temperature profile for different values of Pressure work parameter ε while Pr=0.72 and Ec=0.01.

Values of •	Ec=0.0		Ec=0.05		Ec=0.1		Ec=0.3	
	$f'(\xi,\eta)$	$\theta(\xi,\eta)$	$f'(\xi,\eta)$	$\theta(\xi,\eta)$	$f'(\xi,\eta)$	$\theta(\xi,\eta)$	$f'(\xi,\eta)$	$\theta(\xi,\eta)$
0.00000	0.00000	1.00000	0.00000	1.00000	0.00000	1.00000	0.00000	1.00000
0.05248	0.07623	0.97800	0.07678	0.97963	0.07735	0.98130	0.07974	0.98849
0.10511	0.14962	0.95595	0.15072	0.95900	0.15185	0.96214	0.15663	0.97563
3.50544	1.04686	0.04227	1.04732	0.04270	1.04779	0.04315	1.04965	0.04503
4.01507	1.02034	0.01849	1.02047	0.01865	1.02059	0.01881	1.02107	0.01950
5.39382	1.00018	0.00018	1.00016	0.00017	1.00014	0.00016	1.00005	0.00012

Table 2.5e: Numerical values of the velocity profile and the temperature profile for different values of viscous dissipation parameter Ec while Pr=0.72 and ε =0.01.

Numerical values are presented in the table 2.5f for local skin friction coefficient and local heat transfer rate against • for variation of Prandtl number Pr. Table 2.5g and 2.5h contain the values of the same factors against • for the variation of ε and Ec respectively. The graphical representation of the data are given in the figure 2.5.1(a,b), 2.5.2(a,b), 2.5.3(a,b), 2.5.4(a,b), 2.5.5(a,b), 2.5.6(a,b)

Values of •	Pr=0.3		Pr=0.72		Pr=1.0		Pr=10.0	
	$f''(\xi,0)$	$-\theta'(\xi,0)$	$f''(\xi,0)$	$-\theta'(\xi,0)$	$f''(\xi,0)$	$-\theta'(\xi,0)$	$f''(\xi,0)$	$-\theta'(\xi,0)$
0.00000	0.33205	0.21433	0.33205	0.29438	0.33205	0.33039	0.33205	0.71735
0.02000	0.36828	0.21801	0.36156	0.29890	0.35926	0.33520	0.34658	0.72361
0.10017	0.50181	0.23040	0.47169	0.31452	0.46125	0.35196	0.40252	0.74672
4.83720	4.65225	0.40773	3.96833	0.55099	3.72805	0.61250	2.30482	1.19150
4.93696	4.71960	0.40961	4.02476	0.55346	3.78062	0.61522	2.33409	1.19613
5.24827	4.92732	0.41532	4.19870	0.56098	3.94263	0.62348	2.42385	1.21009

Table2.5f: Numerical values of the local skin friction and the rate of heat transfer for various values of Prandtl number Pr while Ec=0.01and ε =0.01.

Values of •	ε =0.0		ε =0.01		ε =0.04		ε =0.07	
	$f''(\xi,0)$	$-\theta'(\xi,0)$	$f''(\xi,0)$	$-\theta'(\xi,0)$	$f''(\xi,0)$	$-\theta'(\xi,0)$	$f''(\xi,0)$	$-\theta'(\xi,0)$
0.00000	0.33205	0.29438	0.33205	0.29438	0.33205	0.29438	0.33205	0.29438
0.02000	0.36157	0.29881	0.36156	0.29890	0.36154	0.29917	0.36152	0.29944
0.04001	0.39019	0.30296	0.39017	0.30314	0.39009	0.30368	0.39002	0.30422
2.48059	2.54489	0.46258	2.51028	0.47890	2.41665	0.52209	2.33582	0.55840
2.53459	2.58307	0.46423	2.54715	0.48097	2.45020	0.52516	2.36673	0.56217
2.82020	2.78194	0.47249	2.73880	0.49148	2.62363	0.54091	2.52589	0.58157

Table 2.5g: Numerical values of the local skin friction and the rate of heat transfer for various values of Pressure work parameter ε while Pr=0.72 and Ec=0.01.

Values of •	Ec=0.0		Ec=0.05		Ec=0.1		Ec=0.3	
	$f''(\xi,0)$	$-\theta'(\xi,0)$	$f''(\xi,0)$	$-\theta'(\xi,0)$	$f''(\xi,0)$	$-\theta'(\xi,0)$	$f''(\xi,0)$	$-\theta'(\xi,0)$
0.00000	0.33205	0.29563	0.33205	0.28937	0.33205	0.28311	0.33205	0.25807
0.10017	0.47153	0.31615	0.47233	0.30801	0.47314	0.29983	0.47637	0.26678
0.12029	0.49753	0.31967	0.49848	0.31113	0.49944	0.30255	0.50326	0.26778
1.90430	2.09728	0.46580	2.12089	0.40960	2.14548	0.35070	2.25526	0.08336
2.03686	2.19330	0.47251	2.21956	0.41222	2.24700	0.34881	2.37081	0.05807
2.27434	2.36122	0.48397	2.39256	0.41621	2.42551	0.34452	2.57708	0.00943

Table 2.5h: Numerical values of the local skin friction and the rate of heat transfer for various values of viscous dissipation parameter Ec while Pr=0.72 and ε=0.01.

Figure 2.5.1a and 2.5.1b show the velocity and temperature profiles for different values of Prandtl number in presence of the viscous dissipation and pressure work .

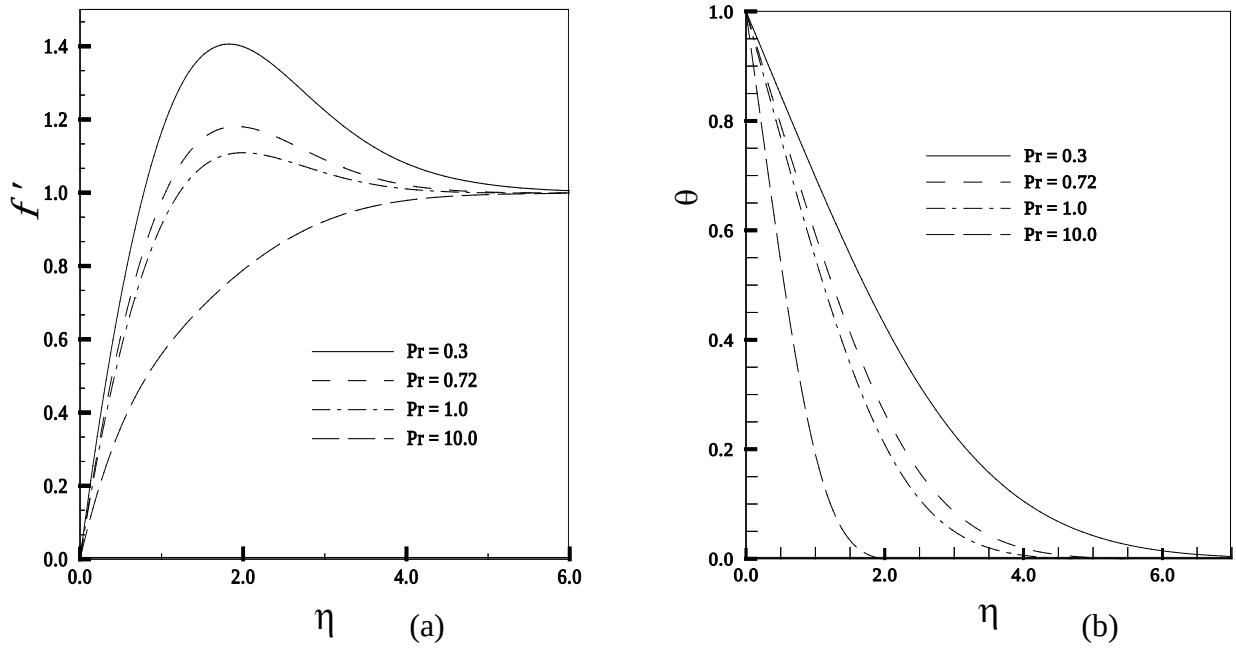

Fig.2.5.1: (a) Velocity and (b) Temperature profiles are shown against • for different values of Prandtl number Pr while Ec=0.01, ε=0.01

From figure 2.5.1a with Prandtl number less than or equal to 1, the velocity in the boundary layer can exceed the external velocity $(f'>1)$ as the buoyancy effect becomes stronger. At Prandtl number greater than 1, the effect of the buoyancy on the velocity profile reduces and we do not

observe any overshoots in the velocity profile as is the case when $\Pr \geq 1$. On the other hand, from figure 2.5.1b we see that the temperature distribution over the whole boundary layer decreases significantly when the values of Prandtl number increases.

The effect of Prandtl number Pr(=0.3, 0.72, 1.0, 10.0) on the local skin friction coefficient and the local heat transfer rate while Ec=0.01 and $\varepsilon = 0.01$ is shown in figure 2.5.2a and 2.5.2b respectively.

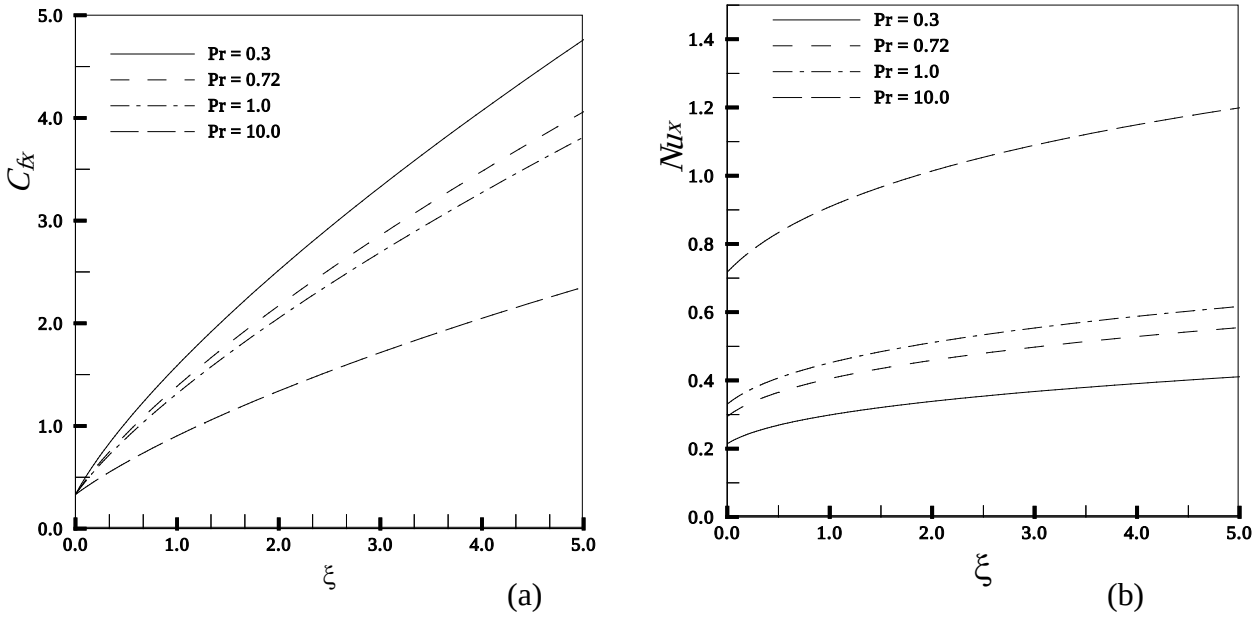

Fig.2.5.2: (a) Skin friction and (b) Rate of heat transfer against • for different values of Prandtl number Pr while Ec=0.01, ε =0.01

It is found that skin friction coefficient decreases and the heat transfer rate increases for increasing values of the Prandtl number Pr. For example, at •=0.2 the values of the skin friction decreases by 28.0968% and the heat transfer rate increases by 215.49% while Pr increasing from 0.3 to 10.0.

Figure 2.5.3a and 2.5.3b illustrate the velocity and temperature profiles for different values of pressure work parameter ε while Pr=0.72 and Ec=0.01.

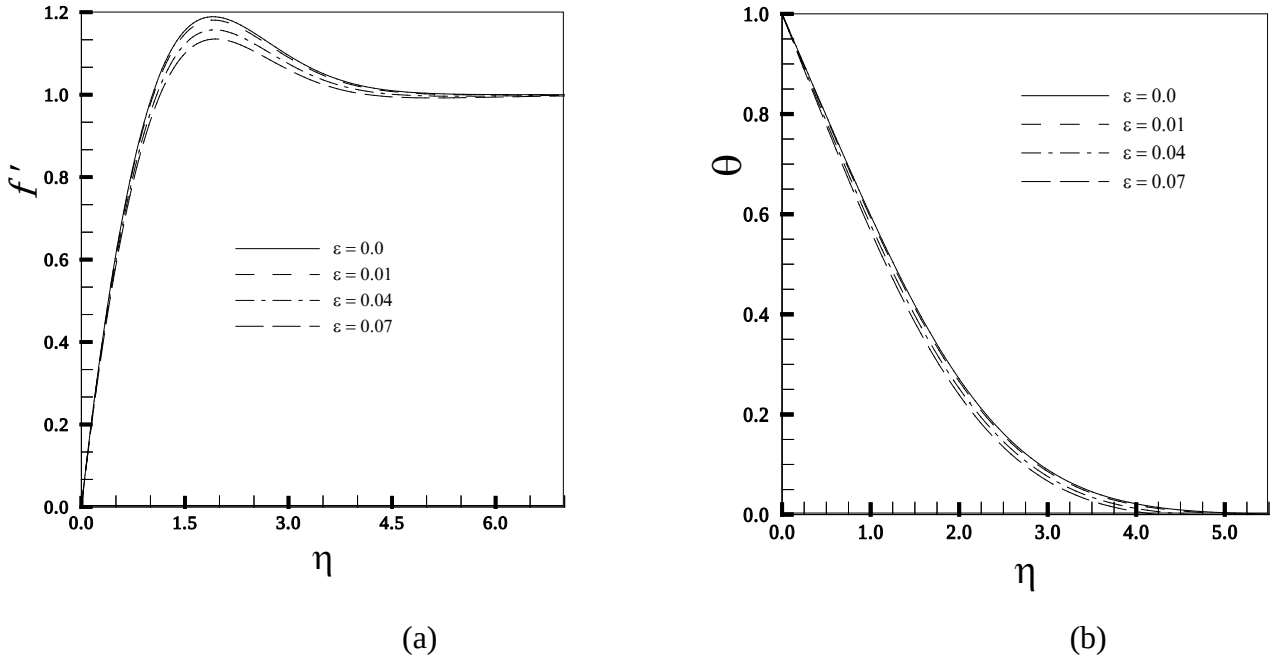

(a) (b)

Fig.2.5.3: (a) Velocity and (b)Temperature profiles are shown against • for different values of Pressure work parameter ε while Pr=0.72, Ec=0.01

We observe from figure 2.5.3a that an increase in the pressure work parameter ε decreases the velocity profiles. But near the surface of the plate the velocity increases , become maximum and then decrease and finally approaches to unity. The maximum values of the velocities are 1.18921, 1.18096, 1.1570, 1.13506 for ε=0.0, 0.01, 0.04, 0.07 respectively occurs at • = 1.88324, 1.93982, 1.99774, 1.93982. Here we find that the velocity decreases by 4.55% as ε increases from 0.0 to 0.07. Clearly it is seen from figure 2.5.3b that the temperature distribution decreases owing to increasing values of the pressure work parameter and becomes maximum at the wall. The local maximum values of the temperature are unity i.e. all are same and become zero as $\eta \to \infty$. But at a particular • >0 decreasing rate is not so much significant.

Figure 2.5.4a and 2.5.4b illustrate the effect of pressure work parameter on the local skin friction coefficient and the local heat transfer rate respectively while Pr=0.72 and Ec=0.01.

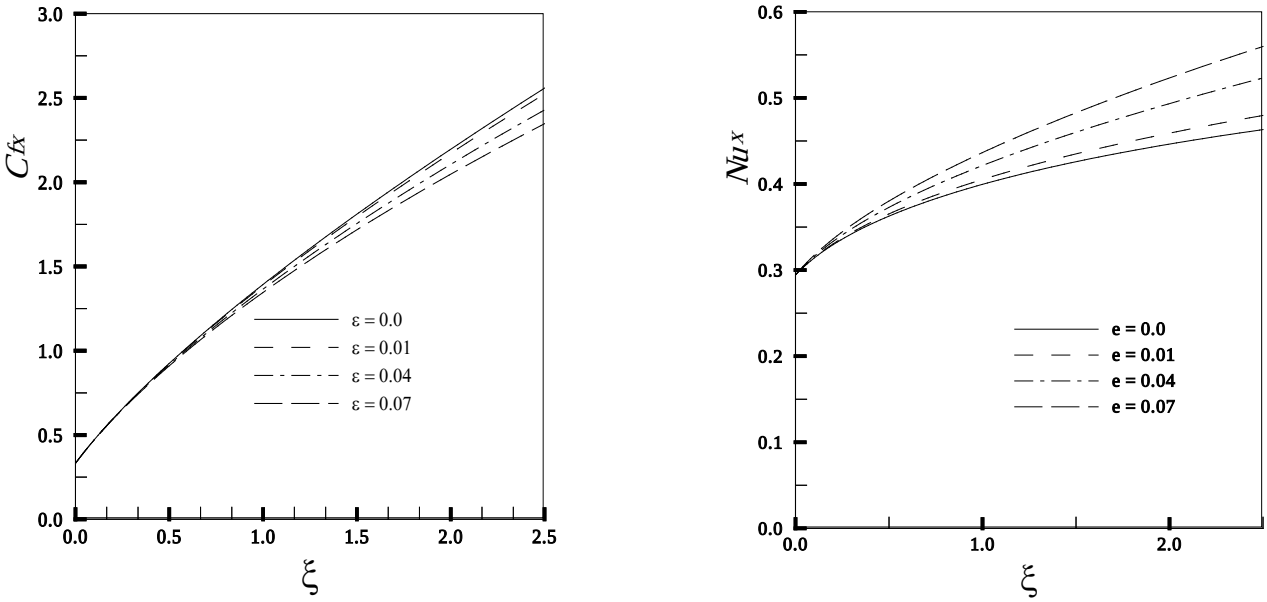

(a) (b)

Fig.2.5.4: (a) Skin friction and (b) Rate of heat transfer against • for different values of Pressure work parameter ε while Pr=0.72, Ec=0.01

From figure 2.5.4a, it is seen that an increase in the pressure work parameter ε (=0.0,0.01,0.04,0.07) leads to a decrease in the local skin friction coefficient and inverse result is observed from figure 2.5.4b for local heat transfer rate.

Figure2.5.5a and 2.5.5b show the effects of the viscous dissipation parameter Ec(=0.0,0.05,0.1,0.3) on the velocity and the temperature profiles for Pr=0.72 and ε =0.01.

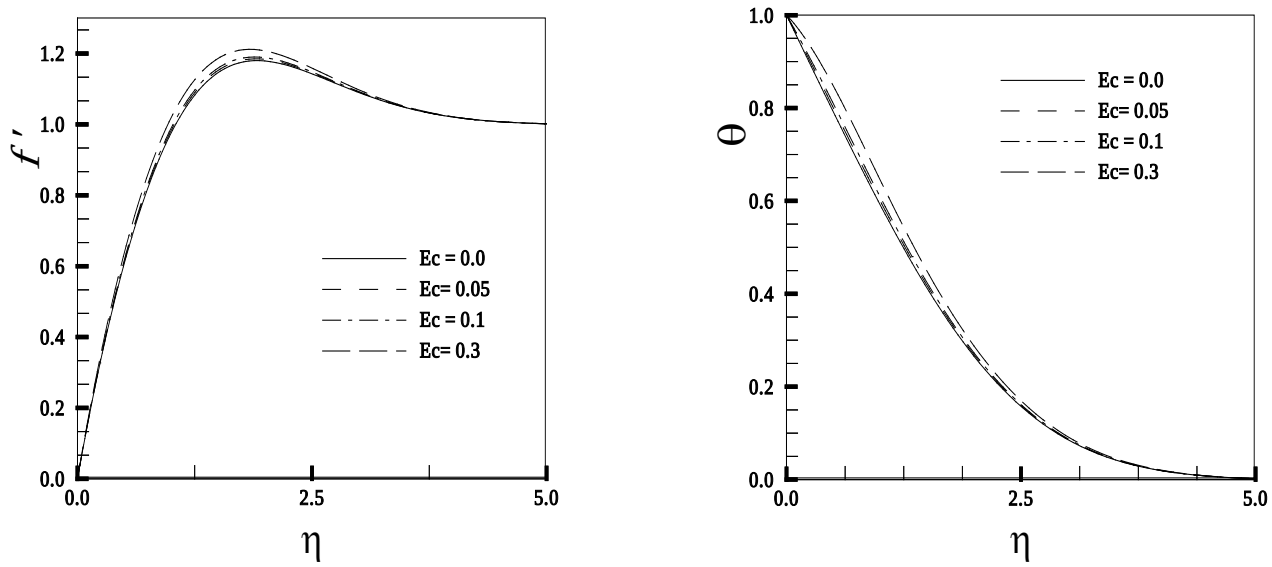

(a) (b)

Fig.2.5.5: (a) Velocity and (b) Temperature profiles are shown against • for different values of viscous dissipation parameter Ec while Pr=0.72, ε =0.01

From figure 2.5.5a, it is revealed that the velocity profile increases with the increase of the viscous dissipation parameter Ec which indicates that viscous dissipation accelerates the fluid motion slightly. In figure 2.5.5b the similar behaviour has also been observed for the temperature profiles with exactly the same values of the parameters Ec, Pr and ε .

Figure 2.5.6a and 2.5.6b show the variation of the local skin friction coefficient and local heat transfer rate with viscous dissipation parameter Ec while Pr=0.72 and ε =0.01.

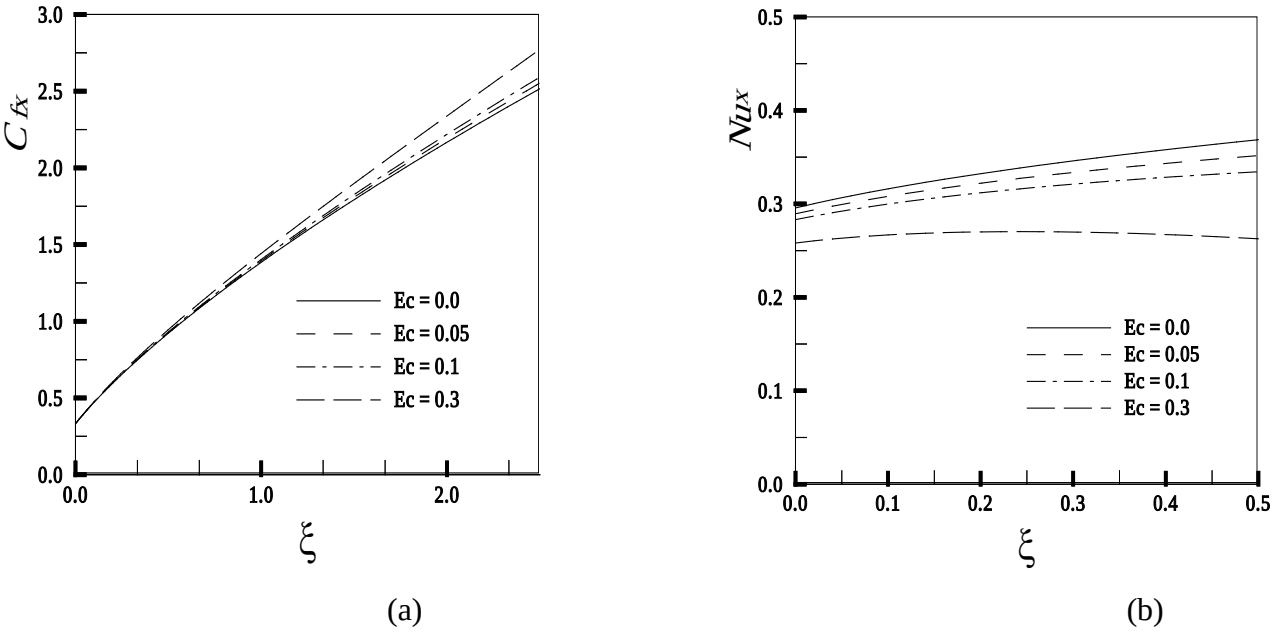

(a) (b)

Fig.2.5.6: (a) Skin friction and (b) Rate of heat transfer against • for different values of Viscous dissipation parameter Ec while Pr=0.72, ε =0.01

It can be seen that the skin friction increases along the • direction for a particular Ec. This is to be expected since the fluid motion within the boundary layer increases for increasing Ec (Fig 2.5.5a) and eventually increases the skin friction factor. Figure 2.5.6b shows that the effect of the viscous dissipation parameter leads to a decrease of the local heat transfer rate.

2.6 Conclusion:

The effect of viscous dissipation and pressure work on mixed convection flow along a vertical isothermal flat plate has been studied. Thermal boundary layer is produced by the sudden increase of the surface temperature of the plate as the motion is started. The results are obtained using a very accurate numerical method, namely the implicit finite difference method. The numerical values of the local skin friction coefficient, local Nusselt number, velocity and temperature profiles have been presented graphically and in tabular form.

We conclude the following from the results and discussions:

- Local skin friction coefficient, velocity and temperature distributions increase and local Nusselt number decrease for increasing values of the viscous dissipation parameter.

- Due to increasing values of the pressure work parameter, local skin friction coefficient, velocity and temperature distributions decrease and the local Nusselt number increase.

- For the increasing values of Prandtl number the values of local skin friction coefficient, velocity and temperature distributions decrease and local Nusselt number increase.

CHAPTER 3

EFFECTS OF PRESSURE STRESS WORK AND VISCOUS DISSIPATION IN MIXED CONVECTION FLOW ALONG A VERTICAL FLAT PLATE IN PRESENCE OF HEAT GENERATION

3.1 Introduction:

The aim of this chapter is to investigate the heat generation effect on mixed convection flow in presence of viscous dissipation and pressure work. The developed governing equations with the associated boundary conditions for this analysis are transferred to dimensionless forms using a local non-similar transformation. The transformed non-linear equations are then solved using the implicit finite difference method along with Newton's linearization approximation. Numerical results are found for different values of the heat generation parameter, viscous dissipation parameter, pressure work parameter with Prandtl number 0.72 which corresponds to air at 250^0K. The overall investigations of the velocity, temperature, skin friction and heat transfer rate are presented graphically.

The study of heat generation or absorption in moving fluids is important in problems dealing with chemical reactions and those concerned with dissociating fluids. Possible heat generation effects may alter the temperature distribution; consequently, the particle deposition rate in nuclear reactors, electronic chips and semiconductor wafers. In fact, the literature is replete with examples dealing with the heat transfer in laminar flow of viscous fluids. Vajravelu and Hadjinolaou [25] studied the heat transfer behavior in the laminar boundary layer for a viscous fluid over a stretching sheet with viscous dissipation and internal heat generation. In this study

the volumetric rate of heat generation was considered as $q''' = Q_o(T - T_\infty)$ for $T \geq T_\infty$ and equal to zero for $T < T_\infty$, where Q_0 is a heat generation constant. Hossain et al. [9] also discussed the problem of natural convection flow along a vertical wavy surface with uniform surface temperature in presence of heat generation. The effects of the conjugate conduction-natural convection heat transfer along a thin vertical plate with non-uniform heat generation have been studied by Mendez and Trevino [19]. Mamun et al.[16] analyzed the heat generation effect on natural convection flow of electrically conducting fluid along a vertical flat plate. Alam et al.[2] studied the effects of thermophoresis and chemical reaction on an unsteady hydromagnetic free convection and mass transfer flow past an impulsively started infinite inclined porous plate in the presence of heat generation or absorption. Teodor Groson [24] showed that the effect of internal heat generation is greater for negative values of the mixed convection parameter on a vertical flat plate embedded in a fluid saturated porus media.

To our best of knowledge, heat generation effect along with viscous dissipation and pressure work on mixed convection flow from an isothermal vertical flat plate has not been studied yet. Here we have focused our attention on the evolution of the surface shear stress in terms of local skin friction and the rate of heat transfer in terms of local Nusselt number, velocity distribution as well as temperature distribution for selected parameters. Heat source accelerates the fluid flow and generates the greater buoyancy force and therefore increases the skin friction factor.

3.2 Geometry of the problem:

Geometry for this problem will be unchanged as we described in chapter one. The appropriate equations for the conservation of mass and momentum correspond to those given by equations (2.2.1) and (2.2.2). To show the effect of heat generation, we write the energy equation (2.2.3) in a slightly different form. The term $\frac{Q_0}{\rho C_p}(T - T_\infty)$ is assumed to be the amount of generated or absorbed heat per unit volume, where Q_0 is constant, which may take as either positive or negative values. When the wall temperature T_s exceeds the free stream temperature T_∞, the

source term represents the heat source when $Q_0 > 0$ and heat sink when $Q_0 < 0$. For the condition that $T_s < T_\infty$ the opposite relationship holds good.

Now the energy equation (2.2.3) takes the following form

$$u\frac{\partial T}{\partial x} + v\frac{\partial T}{\partial y} = \frac{\kappa}{\rho C_P}\frac{\partial^2 T}{\partial y^2} + \frac{\nu}{C_P}\left(\frac{\partial u}{\partial y}\right)^2 + \frac{T\beta}{\rho C_P}u\frac{\partial P}{\partial x} + \frac{Q_0}{\rho C_p}(T - T_\infty) \tag{3.2.1}$$

The governing equations have to be solved along with the same boundary conditions (2.2.4).

3.3 Transformation of the governing equations:

Introducing the same transformations described in section 2.3, into the momentum and energy equations, we obtain the following non linear partial differential equations:

$$f''' + \frac{1}{2}ff'' + \theta\xi = \xi\left(f'\frac{\partial f'}{\partial \xi} - f''\frac{\partial f}{\partial \xi}\right) \tag{3.3.1}$$

$$\frac{1}{\Pr}\theta'' + \frac{1}{2}f\theta' + Ecf''^2 - \varepsilon\xi\left(f'\theta + \frac{T_\infty}{T_s - T_\infty}f'\right) + \xi Q\theta = \xi\left(f'\frac{\partial \theta}{\partial \xi} - \theta'\frac{\partial f}{\partial \xi}\right) \tag{3.3.2}$$

where $Q = \dfrac{Q_0 L^2}{\mu C_p \operatorname{Re} Ri}$ is the heat generation parameter.

In the above equations the primes denote differentiation with respect to $\bullet$.

The corresponding boundary condition takes the form

$$\left.\begin{array}{llll} f = 0, & f' = 0, & \theta = 1 & at\ \ \eta = 0 \\ f' \to 1, & \theta \to 0 & as\ \ \eta \to \infty & \end{array}\right\} \tag{3.3.3}$$

3.4 Solution Methodology:

To get the solutions of the parabolic differential equations (3.3.1) and (3.3.2) along with the boundary condition (3.3.3), we shall employ implicit finite difference method together with Keller- box elimination technique. Since a good description of this method has been discussed in details in Chapter-2, further discussion is disregarded here. The numerical results obtained are presented in the following sections.

3.5 Result and Discussion:

A comprehensive set of numerical results is displayed graphically to illustrate the influence of the various physical parameters on the locally similar solutions. The value of Prandtl number is considered to be 0.72 that correspond to air. Numerical values are presented in the table 3.5a for velocity and temperature profiles for variation of heat generation parameter Q against •. Table 3.5b and 3.5c contain the values of the same factors against • for the variation of ε and Ec respectively.

Values of •	Q=0.01		Q=0.05		Q=0.08		Q=0.1	
	$f'(\xi,\eta)$	$\theta(\xi,\eta)$	$f'(\xi,\eta)$	$\theta(\xi,\eta)$	$f'(\xi,\eta)$	$\theta(\xi,\eta)$	$f'(\xi,\eta)$	$\theta(\xi,\eta)$
0.00000	0.00000	1.00000	0.00000	1.00000	0.00000	1.00000	0.00000	1.00000
0.02623	0.03867	0.98935	0.03919	0.99011	0.03960	0.99069	0.03989	0.99109
0.21138	0.29019	0.91387	0.29437	0.91932	0.29765	0.92356	0.29989	0.92646
3.05619	1.08573	0.08093	1.09024	0.08530	1.09372	0.08876	1.09608	0.09117
4.01507	1.02060	0.01880	1.02156	0.01995	1.02229	0.02087	1.02279	0.02151
5.39382	1.00019	0.00019	1.00023	0.00025	1.00025	0.00030	1.00027	0.00033

Table3.5a: Numerical values of the velocity profile and the temperature profile for different values of heat generation parameter Q while Pr=0.72, Ec=0.01and ε =0.01.

Values of •	ε =0.01		ε =0.05		ε =0.08		ε =0.2	
	$f'(\xi,\eta)$	$\theta(\xi,\eta)$	$f'(\xi,\eta)$	$\theta(\xi,\eta)$	$f'(\xi,\eta)$	$\theta(\xi,\eta)$	$f'(\xi,\eta)$	$\theta(\xi,\eta)$
0.00000	0.00000	1.00000	0.00000	1.00000	0.00000	1.00000	0.00000	1.00000
0.02623	0.03867	0.98935	0.03780	0.98872	0.03719	0.98828	0.03515	0.98682
0.21138	0.29019	0.91387	0.28321	0.90882	0.27840	0.90538	0.26204	0.89388
1.21093	1.07436	0.51713	1.04365	0.49751	1.02234	0.48429	0.94938	0.44116
2.05703	1.18110	0.25434	1.15051	0.23570	1.12898	0.22318	1.05340	0.18286
3.50544	1.04752	0.04295	1.03226	0.03212	1.02109	0.02468	0.97919	0.00004

Table 3.5b: Numerical values of the velocity profile and the temperature profile for different values ofPressure work parameter ε while Pr=0.72, Q=0.01 and Ec=0.01

Values of •	Ec=0.01		Ec=0.05		Ec=0.08		Ec=0.2	
	$f'(\xi,\eta)$	$\theta(\xi,\eta)$	$f'(\xi,\eta)$	$\theta(\xi,\eta)$	$f'(\xi,\eta)$	$\theta(\xi,\eta)$	$f'(\xi,\eta)$	$\theta(\xi,\eta)$
0.00000	0.00000	1.00000	0.00000	1.00000	0.00000	1.00000	0.00000	1.00000
0.02623	0.03867	0.98935	0.03889	0.99003	0.03905	0.99071	0.03977	0.99273
0.21138	0.29019	0.91387	0.29196	0.91822	0.29316	0.92237	0.29888	0.93543
3.05619	1.08573	0.08093	1.08663	0.08167	1.08665	0.08153	1.09007	0.08455
4.01507	1.02060	0.01880	1.02070	0.01893	1.02059	0.01881	1.02106	0.01943
5.39382	1.00019	0.00019	1.00017	0.00018	1.00014	0.00016	1.00010	0.00015

Table 3.5c: Numerical values of the velocity profile and the temperature profile for different values of viscous dissipation parameter Ec while Pr=0.72, Q=0.01 and ε =0.01.

Numerical values are presented in the table 3.5d for local skin friction coefficient and local heat transfer rate against • for variation of heat generation parameter Q. Table 3.5e and 3.5f contain the values of the same factors against • for the variation of ε and Ec respectively. The graphical representation of the data are given in the figure 3.5.1(a,b), 3.5.2(a,b), 3.5.3(a,b), 3.5.4(a,b), 3.5.5(a,b), 3.5.6(a,b)

Values of •	Q=0.01		Q=0.05		Q=0.08		Q=0.1	
	$f''(\xi,0)$	$-\theta'(\xi,0)$	$f''(\xi,0)$	$-\theta'(\xi,0)$	$f''(\xi,0)$	$-\theta'(\xi,0)$	$f''(\xi,0)$	$-\theta'(\xi,0)$
0.00000	0.33205	0.29438	0.33205	0.29438	0.33205	0.29438	0.33205	0.29438
0.02000	0.36157	0.29872	0.36160	0.29800	0.36162	0.29746	0.36164	0.29710
0.20134	0.59809	0.32886	0.59955	0.32233	0.60065	0.31739	0.60140	0.31407
2.03686	2.20971	0.44900	2.25666	0.40071	2.29408	0.36278	2.32011	0.33660
3.00492	2.87885	0.48196	2.95870	0.41551	3.02321	0.36265	3.06865	0.32581
4.10555	3.57177	0.51132	3.69266	0.42567	3.79165	0.35673	3.86210	0.30823

Table 3.5d: Numerical values of the local skin friction and the rate of heat transfer for various values of heat generation parameter Q while Pr=0.72, Ec=0.01and ε =0.0

Values of •	ε =0.01		ε =0.05		ε =0.08		ε =0.2	
	$f''(\xi,0)$	$-\theta'(\xi,0)$	$f''(\xi,0)$	$-\theta'(\xi,0)$	$f''(\xi,0)$	$-\theta'(\xi,0)$	$f''(\xi,0)$	$-\theta'(\xi,0)$
0.00000	0.33205	0.29438	0.33205	0.29438	0.33205	0.29438	0.33205	0.29438
0.02000	0.36157	0.29872	0.36154	0.29908	0.36152	0.29935	0.36143	0.30042
0.20134	0.59809	0.32886	0.59636	0.33270	0.59509	0.33553	0.59017	0.34644
0.78384	1.19755	0.38444	1.17921	0.40102	1.16627	0.41264	1.12041	0.45341
0.80941	1.22096	0.38625	1.20160	0.40342	1.18796	0.41543	1.13977	0.45740
1.17520	1.53988	0.40905	1.50352	0.43483	1.47854	0.45232	1.39430	0.51037

Table 3.5e: Numerical values of the local skin friction and the rate of heat transfer for various values of Pressure work parameter ε while Pr=0.72, Q=0.01 and Ec=0.01.

Values of •	Ec=0.01		Ec=0.05		Ec=0.08		Ec=0.2	
	$f''(\xi,0)$	$-\theta'(\xi,0)$	$f''(\xi,0)$	$-\theta'(\xi,0)$	$f''(\xi,0)$	$-\theta'(\xi,0)$	$f''(\xi,0)$	$-\theta'(\xi,0)$
0.00000	0.33205	0.29438	0.33205	0.28937	0.33205	0.28561	0.33205	0.27059
0.02000	0.36157	0.29872	0.36171	0.29343	0.36182	0.28945	0.36225	0.27353
0.10017	0.47180	0.31367	0.47245	0.30715	0.47293	0.30224	0.47487	0.28249
2.94217	2.83743	0.48007	2.87690	0.40645	2.90799	0.34826	3.04736	0.08490
3.00492	2.87885	0.48196	2.91976	0.40658	2.95201	0.34691	3.09710	0.07604
3.40752	3.13932	0.49347	3.19001	0.40657	3.23031	0.33722	3.41544	0.01555

Table 3.5f: Numerical values of the local skin friction and the rate of heat transfer for various values of viscous dissipation parameter Ec while Pr=0.72, Q=0.01 and ε=0.01.

The increased value of the heat generation parameter Q(=0.01,0.05,0.08,0.1) means that more heat is produced and eventually, that heat accelerates the fluid motion as obtained in figures 3.5.1b and 3.5.1a, respectively.

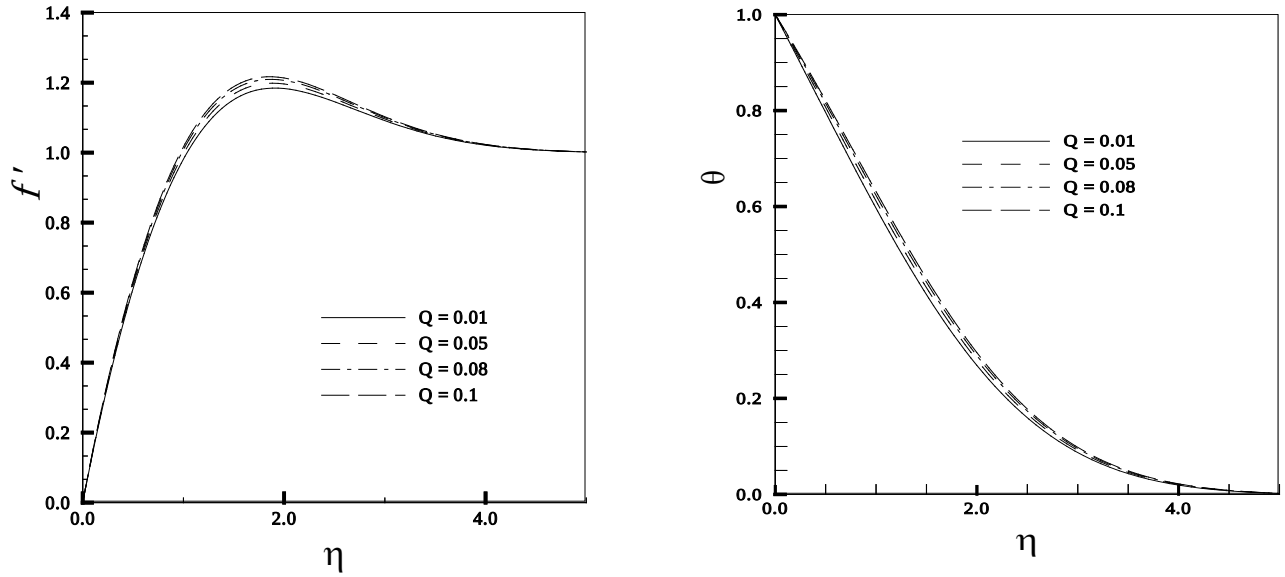

(a) (b)

Fig.3.5.1: (a)Velocity and (b) Temperature profiles are shown against • for different values of heat generation parameter Q while Pr=0.72, Ec=0.01and ε=0.01.

The variation of the local skin friction coefficient and local rate of heat transfer with Ec=0.01 and $\varepsilon = 0.01$ for different values of Q are illustrated in figures 3.5.2a and 3.5.2b, respectively.

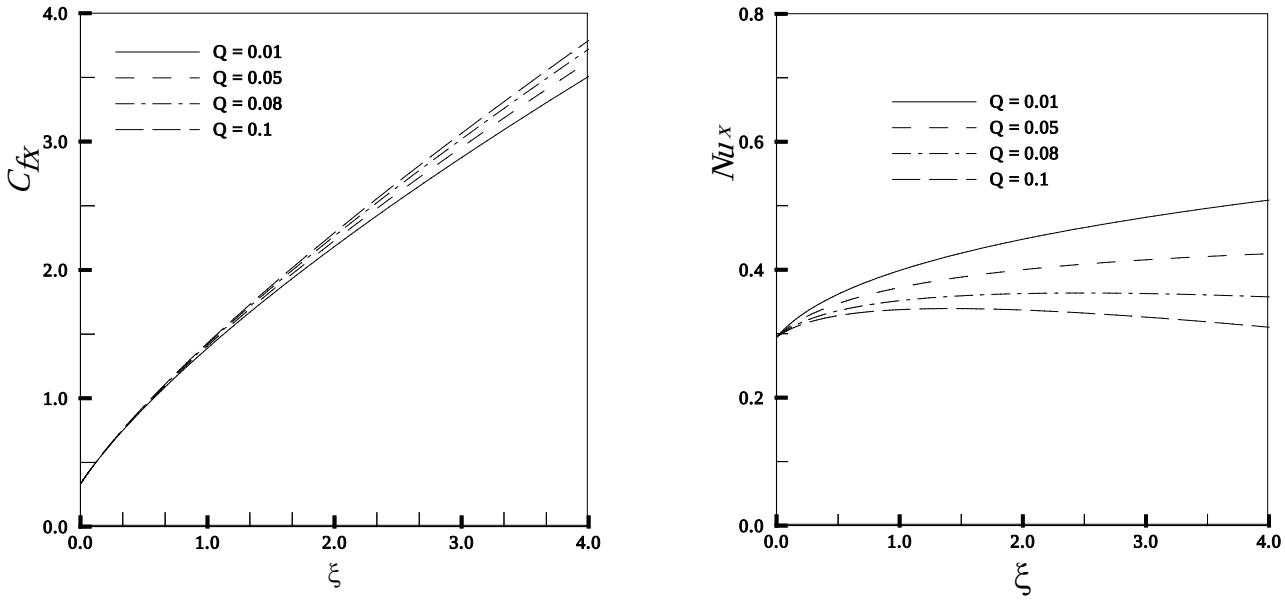

(a) (b)

Fig.3.5.2: (a) Skin friction and (b) Rate of heat transfer against • for different values of heat generation parameter Q while Pr=0.72, Ec=0.01and ε =0.01.

It can be concluded that an increase in the heat generation parameter leads to an increase in the skin friction factor and a decrease in the local heat transfer rate. The heat generation accelerates the fluid flow, as mentioned earlier, and increases the shear stress at the wall. The increased skin friction coefficients with the increasing Q represent this phenomenon as illustrated in figure 3.5.2a.

Moreover, a hot fluid layer is created adjacent to the surface due to the heat generation mechanism As a result, the heat transfer rate from the surface decreases as shown in figure 3.5.2b.

Figure 3.5.3a and 3.5.3b illustrate the velocity and temperature profiles for different values of pressure work parameter ε while Q=0.01 and Ec=0.01.

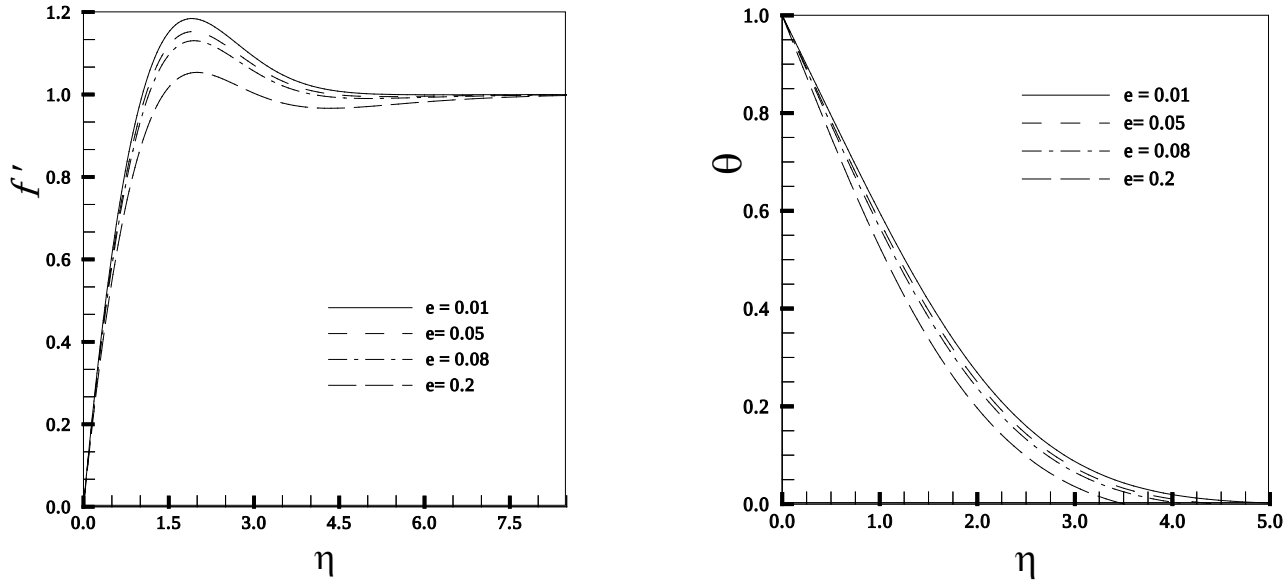

(a) (b)

Fig.3.5.3: (a) Velocity and (b)Temperature profiles are shown against • for different values of Pressure work parameter ε while Pr=0.72, Q=0.01 and Ec=0.01

We observe from figure 3.5.3a that an increase in the pressure work parameter $\in$ decreases the velocity profiles. But near the surface of the plate the velocity increases and become maximum and then decrease and finally approaches to unity. The maximum values of the velocities are 1.18339, 1.15276, 1.13064, 1.05375 for ε=0.01, 0.05, 0.08, 0.2 respectively which occur at • = 1.82795, 1.93982, 1.93982, 1.99774. Here we see that the velocity decreases by 10.95% as ε increases from 0.01 to 0.2. Clearly it is seen from figure 3.5.3b that the temperature distribution decreases owing to increasing values of the pressure work parameter and becomes maximum at the wall. The local maximum values of the temperature are unity i.e. all are same and become zero as $\eta \to \infty$. But at a particular • >0 decreasing rate is significant.

Figure 3.5.4a and 3.5.4b illustrate the effect of pressure work parameter on the local skin friction coefficient and the local heat transfer rate respectively while Q=0.01 and Ec=0.01.

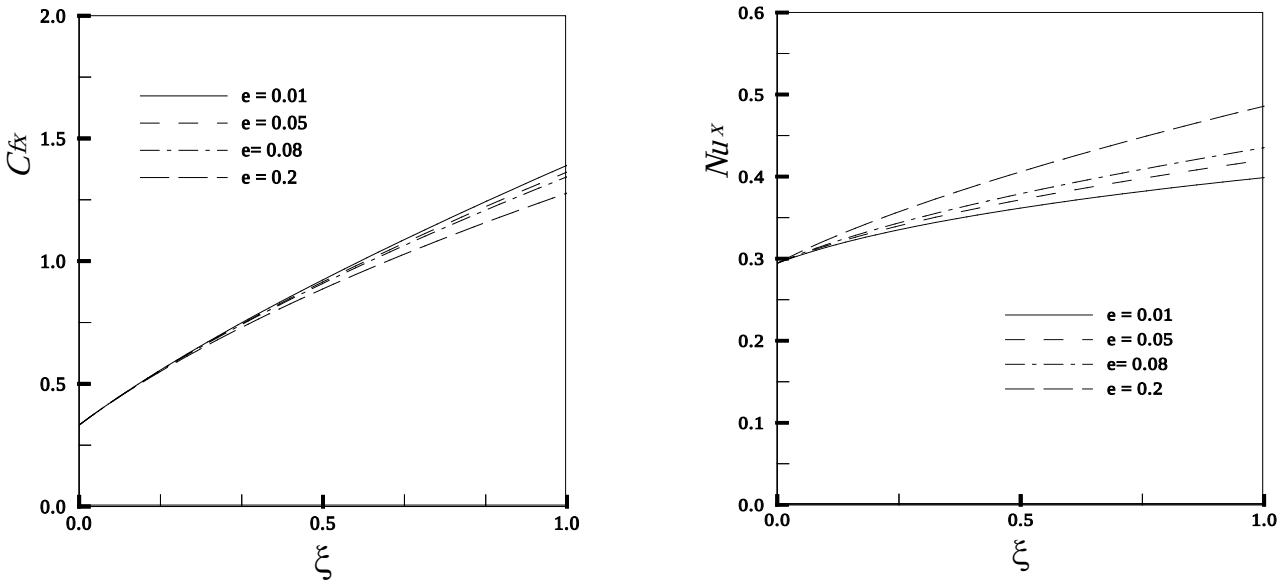

(a) (b)

Fig.3.5.4: (a) Skin friction and (b) Rate of heat transfer against • for different values of Pressure work parameter ε while Pr=0.72, Q=0.01 and Ec=0.01

From figure 3.5.4a, it is seen that an increase in the pressure work parameter ε (=0.01,0.05,0.08,0.2) leads to a decrease in the local skin friction coefficient and inverse result is observed from figure 3.6.4b for local heat transfer rate. This is to be expected since the fluid motion within the boundary layer decreases for increasing ε and eventually decreases the skin friction factor.

Figure3.5.5a and 3.5.5b depict the effects of the viscous dissipation parameter Ec(=0.01,0.05,0.08,0.2) on the velocity and the temperature profiles for Q=0.01 and ε =0.01.

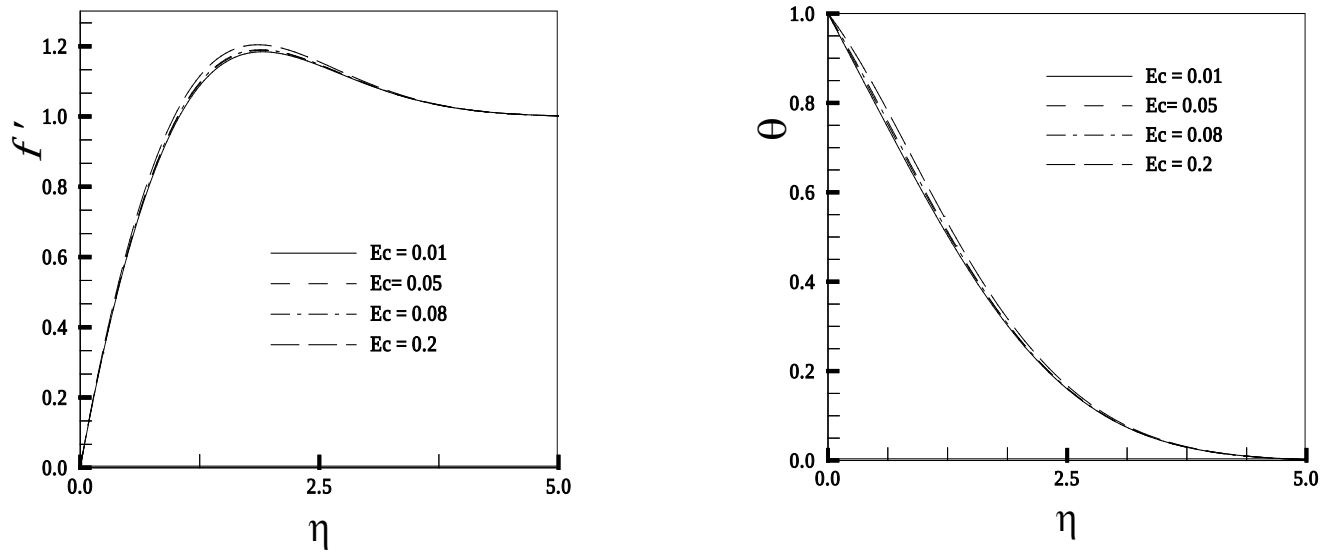

(a) (b)

Fig.3.5.5: (a) Velocity and (b)Temperature profiles are shown against • for different values of viscous dissipation parameter Ec while Pr=0.72, Q=0.01 and ε =0.01.

From figure 3.5.5a, it is revealed that the velocity profile increases with the increase of the viscous dissipation parameter Ec which indicates that viscous dissipation increases the fluid motion slightly. In figure 3.5.5b the similar behaviour has also been observed for the temperature profiles with the similar values of the parameters Ec, Q and ε.

Figure 3.5.6a and 3.5.6b dipict the variation of the local skin friction coefficient and local heat transfer rate with viscous dissipation parameter Ec while Q=0.01and ε =0.01. It can be seen that the skin friction factor increases along the • direction for a particular Ec.

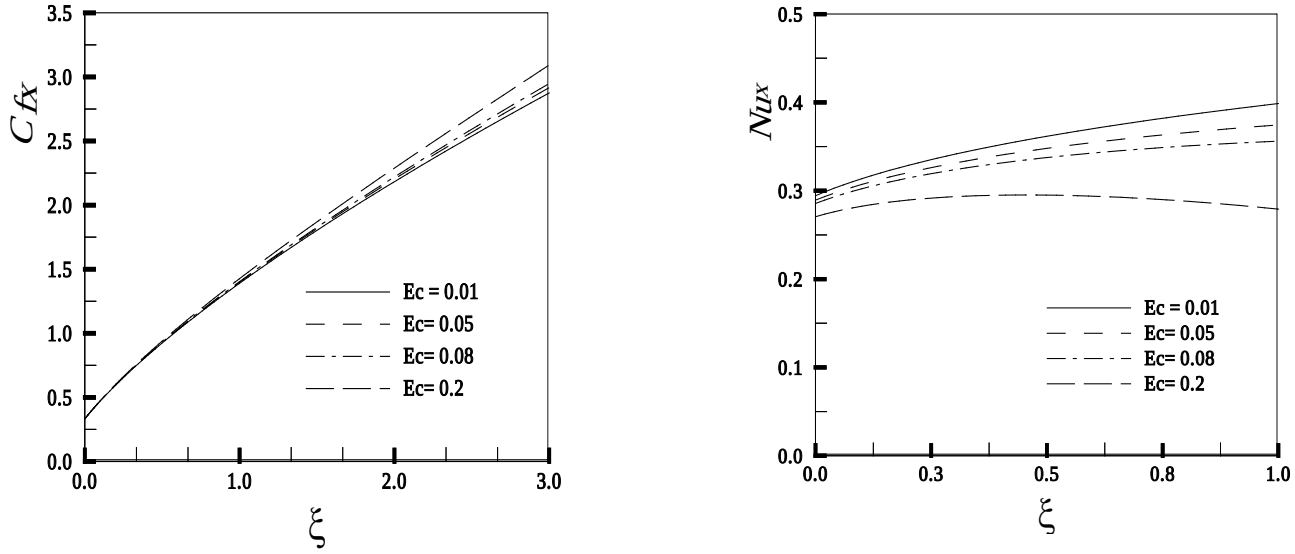

(a) (b)

Fig.3.5.6: (a) Skin friction and (b) Rate of heat transfer against • for different values of Viscous dissipation parameter an=Ec while Pr=0.72, Q=0.01 and ε =0.01

This is to be expected since the fluid motion within the boundary layer increases for increasing Ec (Fig 3.5.6a) and eventually increases the skin friction factor. Figure 3.5.6b shows that the effect of the viscous dissipation parameter leads to decrease the local heat transfer rate.

3.6 Conclusion:

A time independent, two dimensional, laminar mixed convection flow is studied considering heat generation in the presence of viscous dissipation and pressure work effects. The effects of pressure work, viscous dissipation parameter and heat generation parameter are analyzed on the fluid flow. From the present investigation the following conclusion may be drawn.

- The velocity of the fluid and the skin friction at the surface decrease with the increasing pressure work parameter while they increase with the increasing viscous dissipation parameter and heat generation parameter.

- The temperature of the fluid decreases with the increasing pressure work parameter and increases with the increasing viscous dissipation parameter and heat generation parameter.

- The rate of heat transfer increases with the increasing pressure work parameter and decreases with the increasing viscous dissipation parameter and heat generation parameter.

References

[1] Alam, Alim and Chowdhury, 'Effect of pressure stress work and viscous dissipation flow along a vertical flat plate with heat conduction', Journal of Naval Architecture and Marine Engineering, pp 69- 76, December, (2006).

[2] Alam M.S, Rahman M.M., and Sattar M.A., ' Effects of thermophoresis and chemical reaction on an unsteady hydromagnetic free convection and mass transfer flow past an impulsively started infinite inclined porous plate in the presence of heat generation /absorption', Thammasat Int. J. Sc. Tech., Vol. 12, No. 3, pp 44-47. (2007)

[3] Cebeci T., Bradshaw P., 'Physical and Computational Aspects of convective Heat Transfer', Springer, Newyork, (1984)

[4] Gebhart, 'Effect of viscous dissipation in natural convection', J. Fluid Mech., Vol. 14, pp 225-295 (1962).

[5] Gebhart and Mollendorf, ' Viscous dissipation in external natural convection flows'. J. Fluid Mech. S8,pp 97-107 (1969).

[6] Hossain M.A., and Alim M.A., 'Natural convection radiation Interaction on Boundary layer Flow along a Thin cylinder', J. Heat and Mass Transfer, Vol. 32, pp.515-520, (1997)

[7] Hossain and Arbad, 'Forced and Free convection flow with viscous dissipation effects: The method of parametric differentiation', International Atomic Energy Agency and United Nations Educational Scientific and Cultural Organization, International centre for theoretical physics, IC/ 88/ 141.

[8] Hossain M. A., Kutubuddin M., and Takhar H.S., 'Radiation interaction on forced and free convection across a horizontal cylinder', Applied Mechanics and Engineering, Vol. 4, pp.219-235. (1999).

[9] Hossain M.A., Molla M.M., Yao L. S., 'Natural convection flow along a vertical wavy surface with uniform surface temperature in presence of heat generation /absorption', Int. J. Thermal Science, Vol 43, pp. 157–163, (2004).

[10] Hossain, Sidharta and Gorla, 'Unsteady mixed convection boundary layer flow along a symmetric wedge with variable surface temperature', Int. J. Heat and Mass Transfer, Vol 44, pp. 607–620,(2006).

[11] Ishak, Nazar and Pop, 'Mixed convection of the stagnation point flow towards a stretching vertical permeable sheet', Malaysian Journal for Mathematical Sciences 1(2):pp 217-226, (2007).

[12] Ishak, Nazar and Pop, 'Post stagnation point boundary layer flow and mixed convection heat transfer over a vertical linearly stretching sheet', Arch. Mach., Vol 60, pp. 303-322. (2008)

[13] Joshi and Gebhart, 'The effect of pressure stress work and viscous dissipation in some natural convection flows', Int. J. Heat Mass Transfer, Vol 24, No.10, pp 1577- 1588, (1981).

[14] Keller H.B, Cebeci T.,'Accurate Numerical Methods for boundary layer flows , Springer, Newyork, (1971)

[15] Kumari and Nath , 'Development of mixed convection flow over a vertical plate due to an mpulsive motion', Int. J. Heat Mass Transfer, Vol 40, pp 823-828, (2004).

[16] Mamun A.A., Chowdhury Z.R., Azim M.A.,. Maleque M.A., **'**Conjugate Heat Transfer for a Vertical Flat Plate with Heat Generation Effect', Nonlinear Analysis: Modelling and Control, , Vol. 13, No. 2, pp 213–223. (2008)

[17] Mamun A.A., Chowdhury Z.R., Azim M.A., Maleque M.A., ' MHD- conjugate heat transfer analysis for a vertical flat plate in presence of viscous dissipation and heat generation', International Communications in Heat and Mass Transfer, Vol.35, pp 1275- 1280. (2008)

[18] Miyamoto, M., Sumikawa, J., Akiyoshi, T. and Takamura, T., 'The effect of axial heat conduction in a vertical flat plate on free convection heat transfer', Int. J. Heat Mass Transfer, Vol 23, pp 1545- 1553, (1980).

[19] Mendez F., Trevino C., 'The conjugate conduction-natural convection heat transfer along a thin vertical plate with non-uniform internal heat generation', Int. J. Heat and Mass Transfer, Vol 43, pp. 2739–2748,(2000).

[20] Pantokratoras, 'Effect of viscous dissipation and pressure stress work in natural convection along a vertical isothermal plate', Int. J. Heat and Mass Transfer, Vol 46, pp.4979–4983,(2003).

[21] Roslinda Bt Mohd Nazar, 'Mathematical Models for Free and Mixed Convection boundary layer flows of Micropolar fluids', Ph.d thesis, Universiti Teknologi Malaysia, December 2003.

[22] Sachdeva R.C., Fundamentals Engineering heat and Mass Transfer, Wiley Eastern Limited, New Age International Limited, ISBN 81-224-0076-0. (1994)

[23] Soundalgekar V.M., Vighnesan N.V. and Pop I., 'Combined free and forced convection flow past a vertical porous plate', Int. J. Energy Research, Vol.5, pp. 215-226 (1981).

[24] Teodor Groson, 'Mixed convection on a vertical flat plate embedded in a fluid saturated porus media.', J. Engng. Math., Vol 14, pp 301-313. (1980)

[25] Vajravelu K., Hadjinicolaou A., 'Heat transfer in a viscous fluid over a stretching sheet with viscous dissipation and internal heat generation' Int. Commun. Heat Mass transfer, Vol 20, pp 417-430. (1993)

[26] Yao, 'Two-dimensional mixed convection along a flat plate', ASME J. Heat Transfer, Vol 109,pp 440-445, (1987).

[27] Zakerullah, 'Viscous dissipation and pressure work effects in axisymmetric natural convection flows', Ganit (J. Bangladesh Math. Soc.), Vol.2, No. 1, pp 43-51, (1972).

[28] John H Lienhard, 'A Heat Transfer Text Book', Phlogiston Press, Cambridge, Massachusetts, USA, 3rd edition.(2008)

Appendix

Extension of this work

Some proposal related to this problem are given below:

- One may solve this problem considering time dependent flow of the fluid.
- This problem can be extended for the opposed mixed convection flow.
- For the angular flat plate can also be solved.
- Effect of atmospheric pressure on the fluid flow can be shown.